Study on the analytical evaluation of immunoactive sulfated polysaccharides by ligand-assisted nuclear magnetic resonance spectroscopy

朴, 俊夏

https://hdl.handle.net/2324/4496111

出版情報：Kyushu University, 2021, 博士（農学）, 課程博士
バージョン：
権利関係：

Study on the analytical evaluation of immunoactive sulfated polysaccharides by ligand-assisted nuclear magnetic resonance spectroscopy

Juneha Bak

Kyushu University

2021

LIST OF CONTENTS

Chapter III Ligand-assisted nuclear magnetic resonance (NMR) spectrometry assay for sulfate content in sulfated polysaccharides

Abbreviations

- CLSM, confocal laser scanning microscopy
- D_2O, deuterium oxide
- DMSO, dimethyl sulfoxide
- EDC, 1-ethyl-3-(3-dimethylaminopropyl) carbodiimide
- ERK1/2, extracellular regulated kinase 1/2
- EtOH, ethanol
- Gal-*s*, galactose-6-*O*-sulfate
- ICP, inductively coupled plasma
- IFN-γ, interferon-γ
- IL, interleukin
- IS, internal standard
- LOD, limited of detection
- LPS, lipopolysaccharide
- MAPK, mitogen-activated protein kinase
- NB-*s*, neocarrabiose-4-*O*-sulfate
- NK cell, natural killer cell
- NMR, nuclear magnetic resonance
- NO, nitric oxide
- NT-di-*s*, neocarratetraose-41,3-di-*O*-sulfate
- PAMPs, pathogen-associated molecular pattern molecules
- PBS, phosphate buffered saline
- PRRs, pattern-recognition receptors
- qNMR, quantitative NMR
- RF, radiofrequency
- SAPK/JNK, stress-activated protein kinase/c-Jun-*N*-terminal kinase
- SD, standard deviation
- siRNA, small interfering RNA
- TLR, toll-like receptor
- TNF-α, tumor necrosis factor-α
- TSP-d_4, 3-(trimethylsilyl) propionic-2,2,3,3-d_4
- Δδ, change in chemical shift
- δ, chemical shift

Chapter I

Introduction

More than 70 % of the world's surface is covered by oceans, and the marine plants, animals, and microorganisms are used as a vital source of natural products for foods and drugs.[1] Notably, seaweeds are regarded as a food source for coastal countries such as Japan, South Korea, and China, since they are rich in nutrients, including fiber (carbohydrates), proteins, essential fatty acids, vitamins, and minerals.[2,3] Seaweeds are largely categorized according to photosynthetic pigments: red, green, and brown groups.[4] Seaweeds display different compositions from species, while polysaccharides occur in all of them, and represent viscous substance composing of cell walls; among seaweed polysaccharides, carrageenan, ulvan, and fucoidan are the main ones.[5] Because of the characteristic physical properties, seaweed polysaccharides, in particular carrageenan, have been extensively used as natural thickening and stabilizing ingredients in pharmaceuticals, cosmetics, and food industries.[6] In addition to the characteristics of seaweed polysaccharides, recent researches have demonstrated their health benefits in animal[7-11] and human[12-16] studies. Especially, it has been reported that polysaccharides bearing sulfate group, particularly fucoidan, have diverse physiological potentials, such as anti-tumor, anti-cancer, anti-coagulant, and immunostimulatory effects.[7-20]

Fucoidan, a mixture of sulfated polysaccharides with different molecular size of 20–400 kDa,[21,22] is typically present in the “brown” seaweeds such as *Fucus vesiculosus*, *Undaria pinnatifida,* and *Cladosipon okamuranus*.[5,23] The fucoidan backbone is characterized by α(1→3) and/or α(1→4)-linked L-fucose, along with branched moieties of sulfated and/or carboxylated monosaccharides (e.g., fucose, mannose, galactose, glucose, xylose).[24-27] Therefore, structures of seaweed fucoidan vary with species of brown seaweeds, by composition and branched position of monosaccharides.[11,27-29] Fig. 1-1 displays a structure of *F. vesiculosus* fucoidan, having only α(1→3) linked fucose esterified with sulfate group on the C3 and/or C4 positions of fucose.[19] *C. okamuranus*-derived fucoidan possesses slightly complex structure with a repeating of α(1→3) linked fucose and fucose sulfated at C4 position, together with a branched chain of glucuronic acid in every six mole of fucose (Fig. 1-1).[30] The structural diversities of seaweed fucoidan may cause the diverse physiological properties that were mentioned above, while the relationship between structure and physiological effect remains unclear.[11,28,30,31]

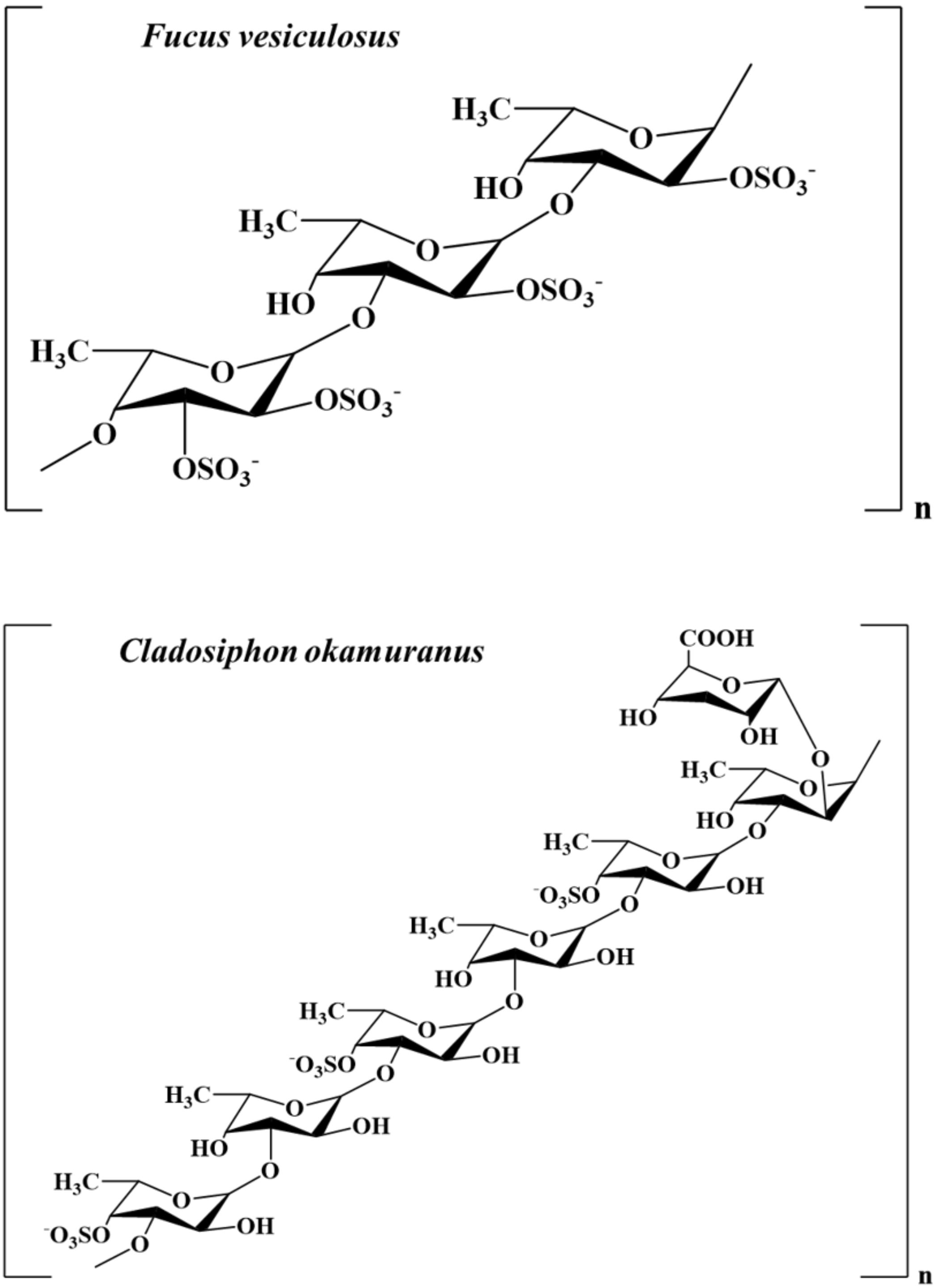

Fig. 1-1. Estimated structure of fucoidan from *Fucus vesiculosus* and *Cladosiphon okamuranus*.

On the other hand, it was reported that the bioactivities of fucoidan are closely associated with the activation of macrophage. Park *et al*.[32] suggested that fucoidan derived from *Hizikia fusiforme* activated a murine macrophage-like cell line, RAW264 cells to produce proinflammatory and tumoricidal molecules such as tumor necrosis factor (TNF)-α and nitric oxide (NO). This result was consistent with that in previous literature reported by Takeda *et al*.,[33] who found that the activated RAW264 cells by *C. okamuranus*-derived fucoidan treatment inhibited the growth of Sarcoma 180 cells with cytocidal action of NO.

Macrophage, classified as innate immune cell, firstly plays an indispensable role to provide immediate defense against foreign pathogens and cancer cells.[34] Notably, the macrophage receptors, termed pattern-recognition receptors (PRRs), including toll-like receptors (TLRs), scavenger receptors, and C-type lectins,[35,36] play a pivotal role in perceiving the invasion of pathogens in a host of macrophage by the recognition of pathogen-associated molecular pattern molecules (PAMPs), such as lipopolysaccharide (LPS) and lipoteichoic acid, expressed on the cell membrane or cell wall of pathogens.[36-38] Since fucoidan is a polyanionic hydrophilic macromolecule, intracellular signals induced by the recognition of fucoidan on cell surface receptors, rather than a cellular internalization, may trigger various bioactivities. In this context, previous studies revealed that PRRs including TLR2, TLR4, scavenger receptors, and C-type lectin-like receptors on macrophage membrane can recognize fucoidan as a foreign substance, resulting in the activation of macrophage.[39-42]

As shown in Fig. 1-2, the recognition of fucoidan on PRRs induces the activation of mitogen-activated protein kinase (MAPK) family including p38 MAPK, extracellular regulated kinase (ERK1/2), and stress-activated protein kinase/c-Jun-*N*-terminal kinase (SAPK/JNK), resulting in activating macrophage.[12,43] In addition to the direct eliminating effect on pathogens and cancer cells, as an important role in augmentation of acquired immune responses, the activated macrophage is known to stimulate other immune cells including T cells by secreting cytokines such as interleukin-12 (IL-12).[44] The activated T cells produce IL-2 and interferon (IFN)-γ, which subsequently induce the proliferation of natural killer (NK) cells. [5] The propagated NK cells attack cancer cell by the secretion of cytokines such as IL-12, TNF-α, and IFN-γ.[45]

Besides, the macrophage activated by multiple ligands recognized by multiple receptors shows much higher physiological activation, in comparison with that activated by a single ligand on a single receptor.[46-48] For example, in human peripheral blood mononuclear cells, the production of TNF-α and IL-10 was promoted by simultaneous treatments with ligands, β-glucan derived from *Alcaligenes faecalis*, Pam3Cys, and LPS for dectin-1, TLR2, and TLR4, respectively.[14] Therefore, co-stimulation of fucoidan together with other ligands such as β-glucan (ligand for dectin-1) and LPS (ligand for TLR4) may possibly show synergistic immune-responses such as immune-stimulation activity.

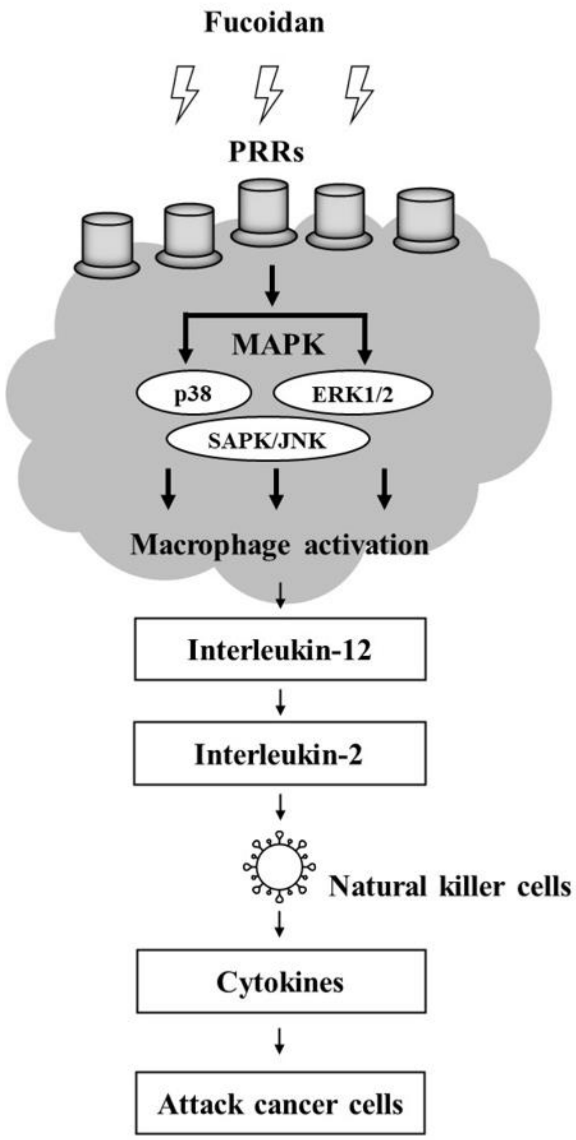

Fig. 1-2. Expected mechanism of fucoidan showing immune-stimulation activity.

Fucoidan, recognized by pattern-recognition receptors (PRRs) expressed on macrophage membrane, stimulates macrophage through activating mitogen-activated protein kinase (MAPK) family including p38 MAPK, extracellular regulated kinase (ERK1/2), and stress-activated protein kinase/c-Jun-*N*-terminal kinase (SAPK/JNK). The activated macrophage ultimately induces the production of cytokines to eliminate cancer cells.

Although the understanding for the detailed mechanism of fucoidan recognition still remains unclear, given an influence of sulfate group on the conformation and the negative net charge of fucoidan,[49-51] the sulfate group is expected to contribute to the fucoidan recognition, resulting in the activation of macrophage.[35] Actually, it has been reported that the presence of sulfate group in fucoidan may be qualitatively and quantitatively associated with the physiological events of fucoidan.[28] The bioactivity of fucoidan seems to be in a sulfate group-dependent manner.[24] For example, fucoidan fraction derived from *Ascophyllum nodosum* containing ca. 27 wt% of sulfate group exhibited much higher anti-coagulant activity compared to fraction with ca. 12 wt% of sulfate group.[25] These results were in line with that in a previous report by Cho *et al*.,[13] who demonstrated that the treatment of *U. pinnatifida*-derived fucoidan in which the hydroxy group was artificially substituted for sulfate group, exerted a stronger anti-cancer effect on a human lung cancer cell line compared to the native fucoidan treatment. However, the lack of information on receptors and on precise sulfate content in polysaccharides still caused poor understanding of fucoidan potential.

A convenient assay commonly conducted to determine the content of sulfate group in polysaccharides uses spectrophotometric method. Namely, after the release of sulfate group with strong acid such as HCl, the released sulfate anions were precipitated with barium ions, followed by the monitoring of the precipitate absorbance at 520 nm.[24,29,50-55] The conventional barium-sulfate assay may suffer from low reproducibility due to its tedious procedures including severe extraction and/or purification, along with the loss of sulfate group and the degradation of polysaccharide structure.[55] Thus, to elucidate the involvement of sulfate group in physiological functions and to control the quality of fucoidan-containing product, a rapid and reliable method for appropriate analytical assay is highly required.[56]

To date, advanced analytical methods using inductively coupled plasma (ICP) spectroscopy, infrared (IR) spectroscopy, and quantitative nuclear magnetic resonance (qNMR) spectroscopy have been developed for sulfate assay of polysaccharides. ICP spectroscopy that shows good selectivity and high sensitivity in biological samples[57] can evaluate the sulfate content according to the equation: %sulfate group= 3.22 × sulfur.[58] However, the ICP technique requires the destructive pretreatments of samples, including acid degradation and exhaustive chemical extraction, causing poor reproducibility.[59,60] IR spectroscopy has been reported for the determination of sulfate content in saccharide, based on the characteristic wave band of 1250–1370 cm^{-1} for sulfate group.[61] However, the application of IR spectroscopy may not be suitable for sulfated polysaccharide assay, due to the overlapping of IR band of polysaccharides (950–1500 cm^{-1})[62] with that of sulfate group.

In contrast to ICP and IR spectroscopies, NMR spectroscopy has been used as powerful, rapid, and straightforward method for structure determination. A recent study also demonstrates an alternative application of NMR, in which NMR can be used as absolute quantitative analytical method in terms of proton number (integrative value) in target, named as qNMR.[63-72] NMR assay is based on the change in behavior of active nuclei by radiofrequency (RF) irradiation in a high magnetic field. Briefly, as shown in Fig. 1-3, positively charged nuclei act like tiny magnet, producing a magnetic dipole with precession. The orientation of nuclear precession occurs in nature with a random orientation, whereas by applying a high external magnetic field, active nuclei are arranged in two orientations, parallel (low energy state) or anti-parallel (high energy state) against the external magnetic field.[73] In a given external magnetic field, irradiation with an equivalent energy to the difference between both energy states of nuclei results in flipping of nuclei spins from low to high energy state, termed "resonance". Since the magnitude of the absorbed frequent light energy is dependent on nuclide and electrons surrounding nuclei, irradiated RF for eliciting resonance corresponds to structural factors of a given chemical.[74] The NMR apparatus expresses the absorbed energy as a free induction decay (FID), which is converted into observable NMR spectrum by the Fourier transform.[75]

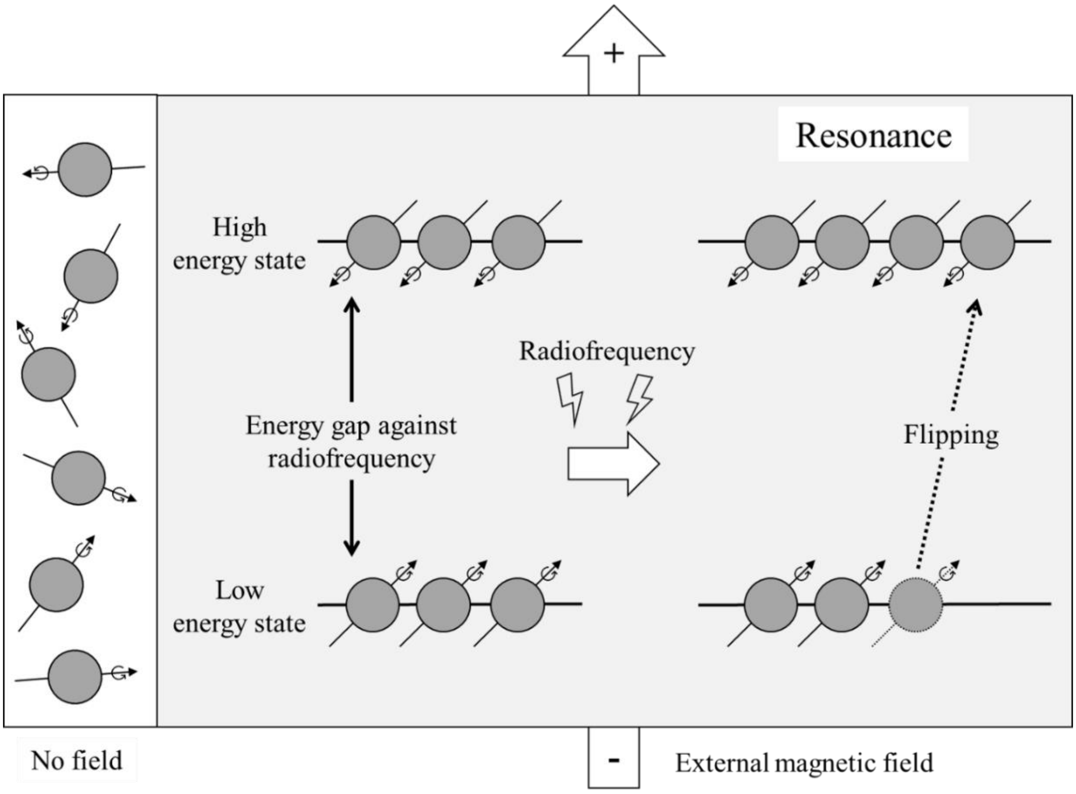

Fig. 1-3. Schematic diagram of nuclear magnetic resonance status for active nuclei with a spin quantum number of 1/2.

Various nuclei such as ^{1}H, ^{13}C, ^{15}N, ^{19}F, ^{31}P, and ^{45}Sc, showing non-zero nuclear spin quantum number, have been used as active nuclei for NMR spectroscopy,[76] among which ^{1}H and ^{13}C NMR spectroscopies are in common to be used for structural analysis.[66] For food analysis, qNMR method[64] has been applied for the evaluation of sugar content in beverages.[67-70] Since the qNMR analysis is based on the quantitative property of ^{1}H nuclei, in which the number of protons in a molecule is proportional to the corresponding ^{1}H NMR signal area,[67] a well-resolved ^{1}H NMR signal of targeting analyte proton is absolutely required. The normalized signal area of analyte target proton by a distinct signal area of internal standard (IS) is used to determine the analyte.[67,77] For example, Berregi *et al.* successfully determined formic acid in apple juice using 1,3,5-benzenetricarboxylic acid as IS.[71] Cao *et al.* determined glucose content in fruit juices using well-resolved anomeric C-1 proton signals of glucose and glucuronic acid as target proton of analyte and IS, respectively.[67] However, in polysaccharide assay, due to busy ^{1}H NMR signals observed in the region of chemical shift (δ) for sugar residues (3.5–5.5 ppm),[70,78] it is extremely hard to identify the characteristic proton signals in sulfated saccharides, including anomeric C-1 protons. Therefore, to evaluate sulfate content in polysaccharides by NMR, an alternative analytical strategy of ^{1}H qNMR method with high selectivity and reliability is needed.

A δ of ^{1}H NMR signal is given as a relative resonance frequency (ppm) of target proton to a reference compound such as 3-(trimethylsilyl)-1-propanesulfonic acid and tetramethylsilane. As the δ value is sensitive to structural changes by any binding interactions such as dipolar interaction, the change in chemical shift ($\Delta\delta$) is monitored to determine a binding site of ligand on a protein.[79,80] Thus far, an NMR titration, observing $\Delta\delta$ of ligand by interaction with a certain anion, has been widely used for designing an artificial receptor for the certain anion.[81-84] For example, Jin *et al*.[84] reported that squaramide-based tripodal receptor dissolved in dimethyl sulfoxide (DMSO) was much more desirable for SO_4^{2-} than $H_2PO_4^-$ by observing δ values of N-H proton in the receptor. Taking into consideration that sulfate group is a strong acid, the phenomena in ionic formation of target sulfate group in polysaccharides with any positive ions may be used for further NMR-guided analytical evaluation.

In general, the observed δ value of ligand by a complex formation between ligand and anion can be expressed as follow:

$$\textbf{Ligand (L)+Anion (A)} \rightleftharpoons \textbf{Complex (C)}$$

$$\begin{aligned}\delta &= (1-n_c)\delta_L + n_c\delta_c \\ &= \delta_L + n_c \times \Delta\delta_{max} \qquad (1)\end{aligned}$$

, where n_c indicates the molar ratio of ligand molecule involved in the complex formation with anion to whole ligand molecule. The δ value of free ligand molecule is shown as δ_L and that of ligand molecule involved in the complex formation with anion is shown as δ_c.

By observing δ values of ligand involved in the stoichiometric complex formation with anion, the molar ratio of ligand to anion can be estimated. For example, if no $\Delta\delta$ of ligand is observed when the molar ratio of ligand to anion is below 1.0, while those of ligand are observed when the molar ratio is over 1.0, it means that the ligand stoichiometrically form 1:1 complex with anion. Therefore, when the observed δ values of ligand proton in the presence of anion (Fig. 1-4A) are schematized against a molar ratio of the ligand to anion (Fig. 1-4B), the molar ratio at the predicted inflection point of the plot clearly corresponds to the stoichiometric complex ratio of ligand to anion.

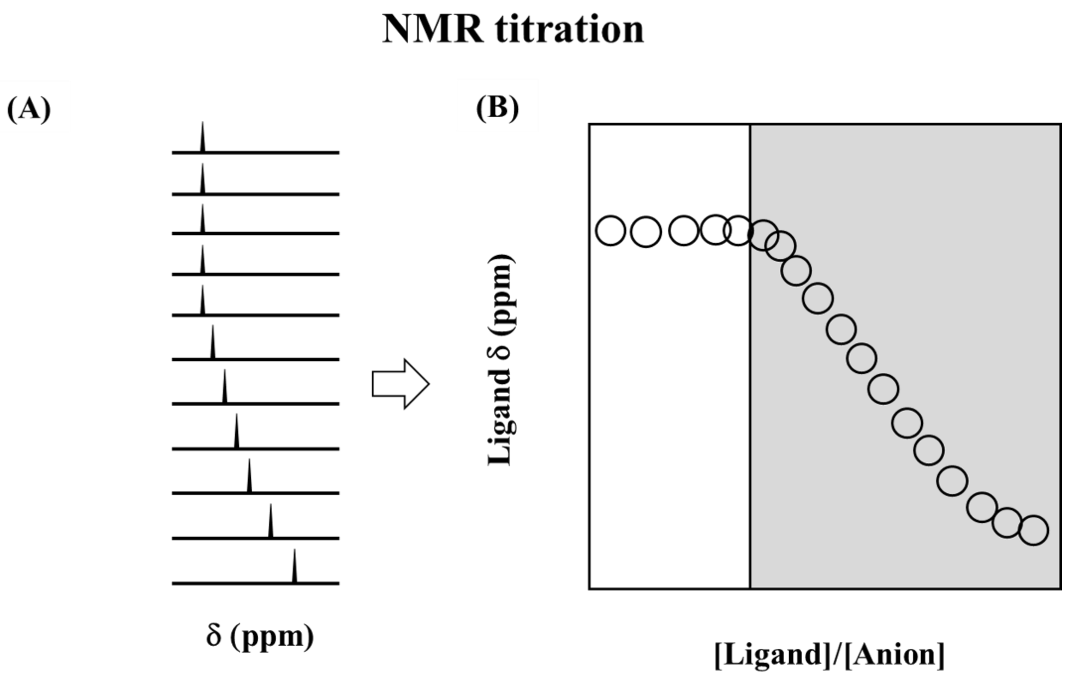

Fig. 1-4. A typical ^{1}H NMR titration curve of a ligand with an anion.

A dose-dependent change in chemical shifts (δ) of ligand target proton in the presence of anion (**A**). Titration profile of δ value of ligand as a function of molar ratio of ligand to anion (**B**). The white-filled area of **B** indicates when whole ligand molecule involves in the complex formation with anion and the gray-filled area of **B** indicates when free ligand molecule coexists with ligand molecule involved in the complex formation.

Additionally, according to the observed δ values of ligand, an associate constant (K) can be estimated. Notably, in archetypal 1:1 binding system, K value is calculated as follows:

$$K = \frac{[C]}{([L]_0-[C])([A]_0-[C])} = \frac{\frac{n_c}{[L]_0}}{(1-n_c)(\frac{[A]_0}{[L]_0}-n_c)} \tag{2}$$

thus,

$$\frac{n_c}{K[L]_0} = (1-n_c)(\frac{[A]_0}{[L]_0}-n_c)$$

or

$$n_c^2 - \left(1+\frac{[A]_0}{[L]_0}+\frac{1}{K[L]_0}\right) \times n_c + \frac{[A]_0}{[L]_0} = 0 \tag{3}$$

$$n_c = \frac{\left(1+\frac{[A]_0}{[L]_0}+\frac{1}{K[L]_0}\right) - \sqrt{\left(1+\frac{[A]_0}{[L]_0}+\frac{1}{K[L]_0}\right)^2 - 4\times\frac{[A]_0}{[L]_0}}}{2} \tag{4}$$

Substituting equation 4 into equation 1 gives

$$\delta = \delta_L + (\Delta\delta_{max}) \times \left[\frac{\left(1+\frac{[A]_0}{[L]_0}+\frac{1}{K[L]_0}\right) - \sqrt{\left(1+\frac{[A]_0}{[L]_0}+\frac{1}{K[L]_0}\right)^2 - 4\mathrm{x}\frac{[A]_0}{[L]_0}}}{2}\right] \tag{5}$$

, where $[L]_0$ and $[A]_0$ are the initial concentrations of ligand and anion, respectively, and [C] is the concentration of complex. Using the 1:1 association model, Khansari *et al.*[82] found that thiourea-based tripodal receptor bearing 3-nitrophenyl groups dissolved in DMSO selectively bound to sulfate anion ($K > 10^{4.0}$ L/mol) rather than other anions such as NO_3^- and I^- ($K < 10$ L/mol). The NMR-estimated K value of sulfate anion to receptor was in good agreement with that in previous literature reported by Jin *et al.*,[84] who suggested that the tris-squaramide receptor dissolved in DMSO-d_6 showed higher binding properties with sulfate group (K of $10^{4.9}$ L/mol) compared to Cl^- (K of $10^{2.6}$ L/mol).

Taken together, when a ligand molecule forming 1:1 stoichiometric complex with sulfate group in saccharides is found by observing $\Delta\delta$ of ligand target proton in the presence of sulfated saccharides, a sulfate content can be estimated from the molar concentration of the ligand at the predicted inflection point of the plot, based on the $\Delta\delta$ of ligand against the molar concentration of ligand (Fig. 1-5). Therefore, to apply the NMR-guided assay for estimating sulfate content in saccharides including natural polysaccharides, the selection of an appropriate ligand, which can form the 1:1 stoichiometric complex with sulfate group in saccharides, is absolutely prioritized. Compounds containing azacyclic, ammonium, and/or guanidinium groups, reported in pervious literatures to show high binding affinity with sulfate anion, are expected to be promising ligand candidates.[82-88]

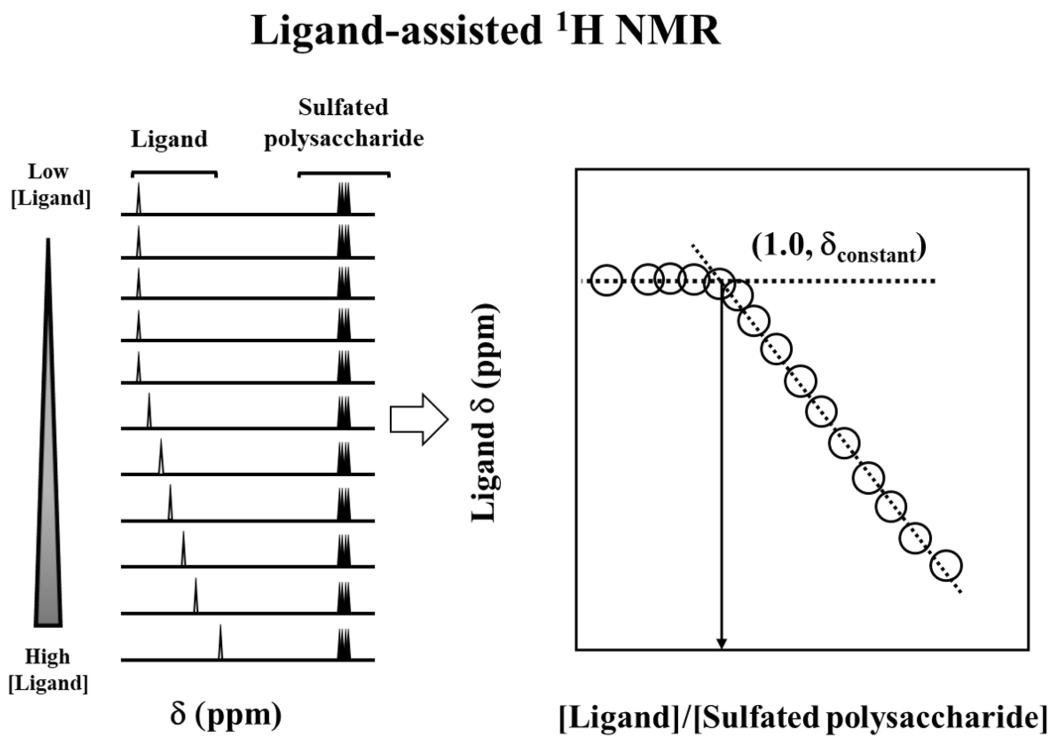

Fig. 1-5. An overview of ligand-assisted ^{1}H NMR assay to estimate sulfate content in sulfated polysaccharides.

In 1:1 binding system of ligand with sulfate group in sulfated polysaccharides, since the observed chemical shift (δ) value of ligand target proton is constant until the molar ratio of ligand to sulfate group is over 1.0, the molar concentration of ligand at the predicted inflection point from the regression equation clearly corresponds to sulfate content in sulfated polysaccharides.

According to the aforementioned research background, while the sulfate group may play important roles in the expression of physiological activities of fucoidan, the understanding of the structural and physical mechanisms of action is still unclear. To understand the relationship between the sulfate group and bioactivities, a reliable analytical assay system which can evaluate sulfate content in polysaccharides without destructive processes (e.g., acid-based treatment) is required. To date, the sulfate group in fucoidan is regarded as a crucial structural factor in interaction with any receptors such as PRRs expressed on macrophage membrane. In addition, it is expected that fucoidan cooperates with other ligands such as β-glucan (ligand for dectin-1) to stimulate multiple receptors, and enhances immunostimulatory function through the activation of macrophage. Therefore, the present study performed with two different aspects as follows:

In **Chapter II**, the immunostimulatory effect of *C. okamuranus*-derived fucoidan on the activation of macrophage and the manner of action was investigated using RAW264 cells. Additionally, to explore the synergistic effect of fucoidan with β-glucan on macrophage activation, RAW264 cells were co-treated with fucoidan and zymosan, a well-known β-glucan-rich cell wall prepared from *Saccharomyces cerevisiae*.

In **Chapter III,** to establish a ligand-assisted ^{1}H NMR assay for estimating sulfate content in polysaccharides, firstly, a suitable ligand molecule forming the stoichiometric complex with sulfate group in sulfated saccharides was selected by screening various candidates. Secondly, sulfate content in commercially available fucoidan derived from *F. vesiculosus* was evaluated by the novel assay. Lastly, for extensive application of the proposed ^{1}H NMR-based assay, twenty crude polysaccharides were extracted from edible seaweeds dealt in market, and their sulfate contents were estimated. To confirm the accuracy of the proposed ligand-assisted ^{1}H NMR assay, estimated sulfate content values were compared by those from a conventional barium-rhodizonate assay.

Chapter II

Synergistic immune-stimulation on macrophage activation by Okinawa-Mozuku (*Cladosiphon okamuranus*) fucoidan and β-glucan derived from *Saccharomyces cerevisiae* in RAW264 cells

1. Introduction

Fucoidan is a crude sulfated polysaccharide which occurs in an extracellular matrix of brown seaweeds such as Okinawa-Mozuku (*C. okamuranus*) and Mekabu (*U. pinnatifida*).[5] Naturally occurring fucoidan displays diverse sulfated polysaccharide forms composed of different monosaccharides (fucose, mannose, galactose, glucose, or xylose, etc.) depending on the species of brown seaweeds.[18,89] For instance, *C. okamuranus* fucoidan is composed of fucose, glucuronic acid, and sulfate with a molar ratio of 6 : 1 : 3 in monomeric unit, having a linear backbone structure of α(1→3) linked fucopyranose, in which glucuronic acid is positioned at C-2 and sulfate is positioned at C-4.[30] Irrespective to the structural diversity of fucoidan, these polysaccharides exhibited several physiological functions, such as anti-tumor, anti-cancer, and anti-inflammatory effects, that are characteristic for sulfated saccharides, but not for non-sulfated ones.[49,51,90,91]

The fucoidan-induced effects regarding immune responses were closely associated with the action of macrophage, categorized as an innate immune cell, playing a requisite role in protecting its host from exotic pathogens.[34] Thus far, it has been reported that fucoidan has the ability to activate macrophage through the agonistic binding to PRRs expressed on cell membrane, including TLRs and scavenger receptors.[40-42] Then, the fucoidan-stimulated macrophage can induce type 1 helper T cell immune responses and cause activation and expansion of NK cells to eliminate pathogens and cancer cells.[92,93] However, the mode of action of fucoidan to activate immune cells, especially macrophage, has not been well clarified yet.

Notably, the macrophage activated by simultaneous stimulation of multiple receptors expressed on the cell membrane exhibited much powerful immune responses compared to those from single receptor stimulation. For example, in RAW264 cells and human peripheral blood mononuclear cells, the production of proinflammatory molecules including NO and TNF-α was elevated when dectin-1, a well-known β-glucan receptor classified into C-type lectin, was further activated together with both TLR2 and TLR4.[14,94] Simultaneous stimulation by fucoidan (ligand for TLRs or unidentified receptors) and β-glucan (ligand for dectin-1) is expected to synergistically enhance the activation of macrophage.

Therefore, in this study, the immunostimulatory mechanism of *C. okamuranus*-derived fucoidan, and immune-synergistic effect of the co-stimulation by fucoidan together with zymosan, derived from β-glucan-rich *S. cerevisiae* cell wall, on the activation of macrophage were investigated.

2. Materials and Methods

2.1. Materials

Spray-dried *C. okamuranus*-derived fucoidan (>70% purity and MW>10,000) was provided from the non-profit organization Research Institute of Fucoidan (Fukuoka, Japan). Zymosan (ligand for dectin-1 and TLR2)[94] and depleted zymosan (a hot alkali-treated zymosan; ligand for dectin-1)[94] derived from *S. cerevisiae*, and ligands for TLRs (a Mouse TLR1-9 Ligand Kit) were purchased from InvivoGen (SanDiego, CA). Griess reagent kit (NK05) for estimating the production of NO and biotin hydrazide were obtained from Dojindo Lab. (Kumamoto, Japan). CF568-conjugated streptavidin was purchased from Biotium Inc. (Fremont, CA). Cytochalasin D and methyl β-cyclodextrin were gained from Sigma-Aldrich (St Louis, MO). Phagocytosis Assay Kit (IgG FITC) was obtained from Cayman Chemical (Ann Arbor, MI). For knockdown experiments, HiPerFect Transfection Reagent and small interfering RNAs (siRNAs) (dectin-1: sc-63277 and control: sc-37007) were purchased from Qiagen (Hilden, Germany) and SantaCruz Biotechnology (Dallas, TX), respectively. ELISA kit for TNF-α (88-7324), and WST-8 (07553-44) were obtained from Thermo Fisher Scientific Inc. (Waltham, MA) and Nacalai Tesque Inc. (Kyoto, Japan), respectively.

2.2. Preparation of biotin-conjugated fucoidan

A biotin-conjugated fucoidan was prepared with biotin hydrazide. Firstly, 1 mL of fucoidan solution (4 mg/mL in 0.5 mol/L sodium acetate buffer, pH 5.5) was treated overnight with 1 mL of 20 mmol/L sodium meta-periodate at 4°C to generate aldehyde groups in polysaccharide terminal residues. The mixture then underwent desalting process with PD-10 column (14.5 × 50 mm; GE Healthcare; Freiburg, Germany) according to the manufacturer's recommended protocol, and 0.1 mg biotin hydrazide was added. After 2 h incubation at room temperature in the dark, the reactant was desalted with PD-10 column. The filtrate was lyophilized and weighed. Prior to assay, the dried biotin-conjugated fucoidan was dissolved in phosphate buffered saline (PBS) to 20 mg/mL.

2.3. Cell culture

Murine macrophage-like cell line, RAW264, was purchased from Riken Cell Bank (Tsukuba, Japan). RAW264 cells (2×10^4 cells/200 μL/well) were seeded in 96-well culture plates with Roswell Park Memorial Institute (RPMI) 1640 medium containing 5% fetal bovine serum (FBS). The cells were incubated in a normal humidified atmospheric incubator (containing 95% air and 5% CO_2) at 37°C for 24 h prior to stimulation. After incubation, to evaluate synergistic immunoactivity of the *C. okamuranus*-derived fucoidan with either zymosan or ligands for TLRs, the cells were stimulated with 200 μL of sample mixtures dissolved in the culture medium containing fucoidan (10 μg/mL) and zymosan (0–500 ng/mL) or ligands for TLRs. The ligands for TLRs were prepared at the following concentrations; 2.5 ng/mL Pam3CSK4 (ligand for TLR1/2), 12.5×10^6 cells/mL heat-killed *Listeria monocytogenes* (HKLM, ligand for TLR2), 250 ng/mL Poly (I:C) (ligand for TLR3), 500 pg/mL LPS (ligand for TLR4), 250 ng/mL FLA-ST (ligand for TLR5), and 500 pg/mL FSL-1 (ligand for TLR6/2). For evaluating that fucoidan binds to the plasma membrane to activate macrophage, RAW264 cells were pretreated with 3 mmol/L methyl β-cyclodextrin (used for disrupting lipid rafts via pulling out cholesterol from cell membrance)[95] or 5 μg/mL cytochalasin D (used for inhibiting phagocytosis)[96] for 0.5 or 1 h, respectively, prior to co-stimulation by fucoidan and zymosan. Cell viability and production of NO and TNF-α in the culture supernatants were measured at 24 h after the treatment using WST-8, Griess reagent kit, and ELISA kit, respectively.

2.4. Confocal laser scanning microscopy (CLSM)

To investigate the location of fucoidan in RAW264 cells, the cells (2×10^4 cells/200 μL/well) were seeded in multi-well glass bottom dishes (Matsunami Glass Ind., Osaka, Japan) and incubated under normal culture conditions (humidified atmosphere containing 95% air and 5% CO_2) at 37°C for 24 h. After incubation, the cells were pretreated with 100 μL of 5 μg/mL cytochalasin D for 1 h at 37°C to inhibit phagocytosis of RAW264 cells. Then, the cells were stimulated with 100 μL of 2 mg/mL biotin-conjugated fucoidan for 10 min on ice and washed with ice-cold PBS. Subsequently, cells were treated with CF568-conjugated streptavidin, either immediately or after 3 h incubation at 37°C, for localizing biotin-conjugated fucoidan. Simultaneously, the ability of phagocytosis of the RAW264 cells were evaluated with Phagocytosis Assay Kit (IgG FITC) according to the manufacturer's recommendations. To observe the location of fluorescent-labeled fucoidan on cells, a confocal laser scanning microscope (TCS SP8, Leica, Germany) and LAS X software (Leica) were used.

2.5. siRNA transfection of dectin-1 gene in RAW264 cells

RAW264 cells (5×10^4 cells/well) were seeded in a 24-well culture plate in 100 μL of RPMI1640 medium and transfected with dectin-1 or non-targeting siRNA (50 nmol/L). Briefly, siRNA was diluted with Opti-MEM (Life Technologies, Gaithersburg, MD, USA) and HiPerFect transfection reagent (QIAGEN), and incubated under normal culture conditions for 6 h at 37°C. After incubation, 400 μL of RPMI1640 medium containing 10% FBS was added to each well, followed by the re-incubation under the same culture conditions for 72 h. To evaluate gene knockdown efficiency in RAW264 cells, a quantitative-real time PCR was performed with primers for *clec7a* (gene for dectin-1) and Mx3000P real-time QPCR system (Agilent Technologies, Santa Clara, CA).

2.6. Statistical analysis

All data are shown as the mean ± standard deviation (SD). For comparing each of experimental value to non-treated control, unpaired Student's *t*-test was used. One-way analysis of variance followed by Tukey-Kramer test for *post hoc* analysis was used for multiple comparisons. A p value of <0.05 was considered to be statistically significant.

3. Results and Discussion

3.1 Interaction of fucoidan with RAW264 cell membranes

Macrophage is an immune cell with phagocytic ability to eliminate pathogens. At first, to verify if an internalization of fucoidan into macrophage through the phagocytosis is involved in the activation of macrophage, RAW264 cells pretreated with cytochalasin D, an inhibitor of phagocytosis, were treated with fucoidan. As shown in Fig. 2-1, a decline of green fluorescence intensity (FI) (upper right) was observed without significant cytotoxicity (upper left), indicating that cytochalasin D treatment effectively blocked the internalization of FITC-conjugated latex beads by phagocytosis. Furthermore, irrespective to the phagocytic ability, fucoidan stimulated RAW264 cells to produce much more NO and TNF-α compared to non-fucoidan-treated control (Fig. 2-1 lower left and right). Therefore, it was suggested that fucoidan can exert immune-stimulation activity without phagocytic internalization by macrophage.

Next, to investigate the location of the interaction of fucoidan with RAW264 cells, the cells were treated with biotin-conjugated fucoidan, followed by staining with CF568-conjugated streptavidin. CLSM was used for the visualization of fucoidan (red) and FITC-conjugated latex beads (green).[96] As shown in Fig. 2-2, fucoidan was localized in a dot-like pattern along the cell membrane, under the different experimental conditions.

From these results, it was suggested that some receptors expressed on the cell membrane recognized fucoidan to activate RAW264 cells.[33,41,43] While receptors for *C. okamuranus*-derived fucoidan in RAW264 cells have not been identified so far, a few PRRs expressed on macrophage membranes such as TLR2, TLR4, and scavenger receptor-A are expected to be possible fucoidan receptors.[43,97]

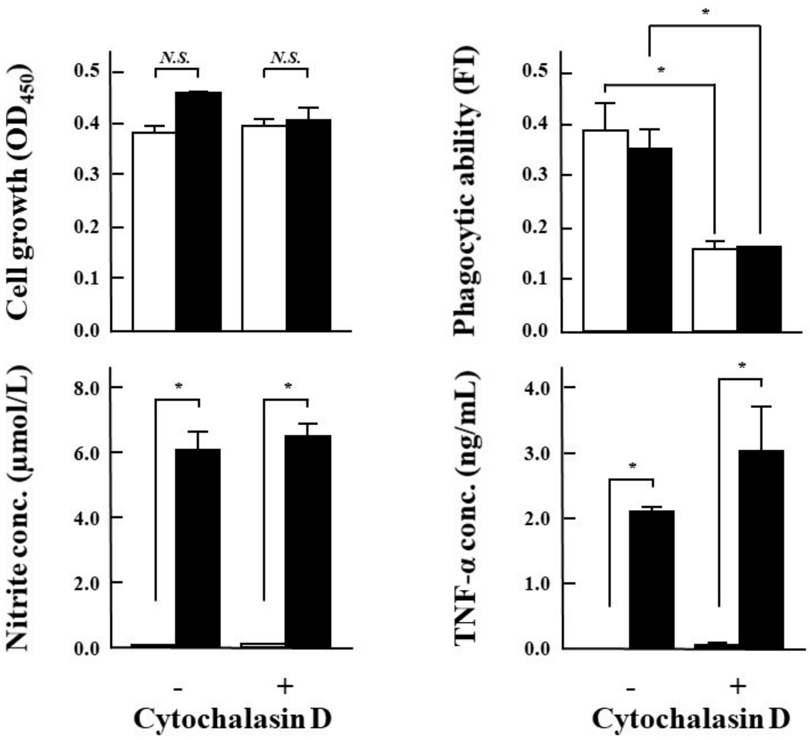

Fig. 2-1. Effect of phagocytic ability on immune-stimulation activity of fucoidan.

Five µg/mL cytochalasin D-pretreated RAW264 cells were activated with 0 (open column) or 10 µg/mL (closed column) fucoidan. Data were shown as the mean ± SD. Each of experimental value of phagocytic ability in cytochalasin D-pretreated RAW264 cells with or without fucoidan treatment was compared to those in cytochalasin D-non-pretreated cells with or without fucoidan treatment, respectively. Each of the experimental values of cytotoxicity and production of NO and TNF-α with fucoidan treatment (closed column) were compared to those of fucoidan-non-treated control (open column). Statistical difference was evaluated by unpaired Student's *t*-test. Asterisk (*) mark on column indicates the significant difference compared to non-treated control (p<0.05, n=4). N.S. indicates no significance.

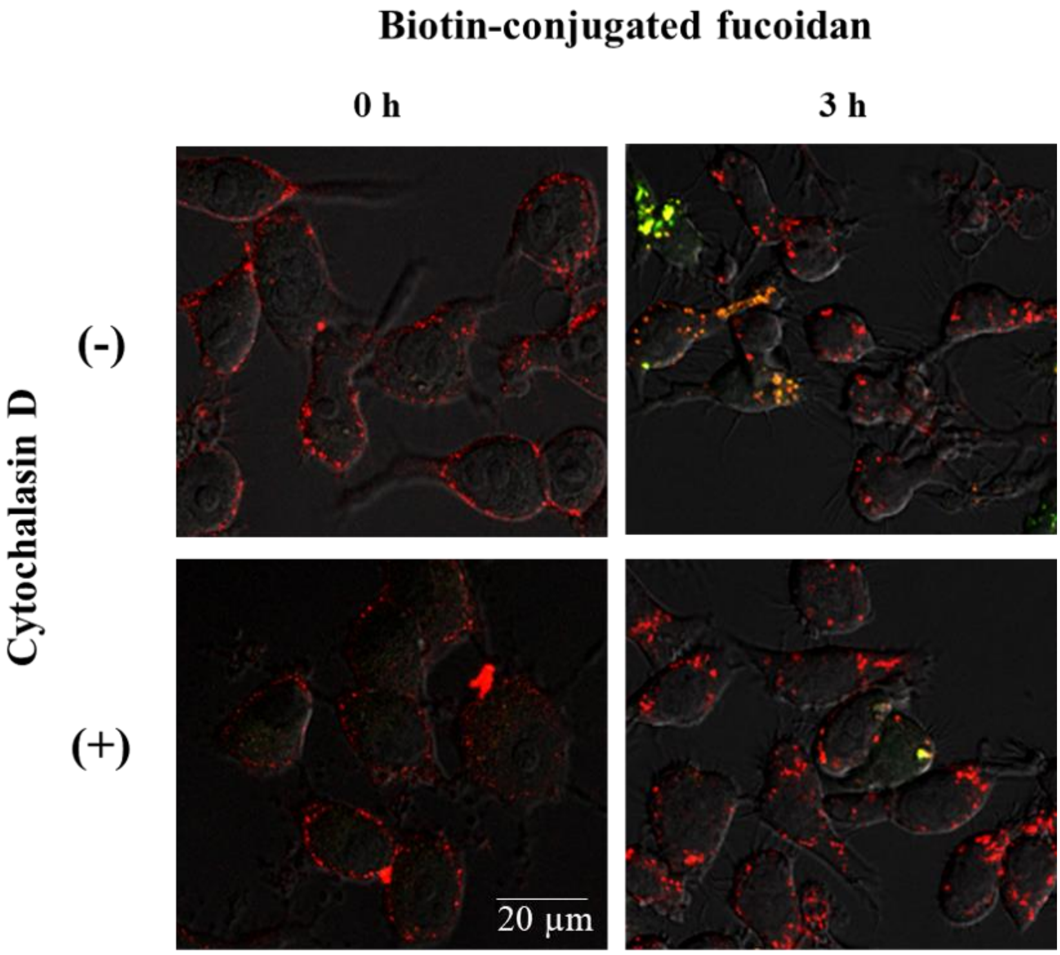

Fig. 2-2. Location of fucoidan on RAW264 cells.

Biotin-conjugated fucoidan was synthesized as stated in the section of Materials and Methods. RAW264 cells were treated with cytochalasin D to block phagocytosis. FITC-conjugated latex beads (Green) for evaluating phagocytic level and biotin-conjugated fucoidan were treated to cytochalasin D-treated RAW264 cells. To stain fucoidan, Cells were treated with CF®568-conjugated streptavidin (Red) either immediately or 3 h after incubation, followed by CLSM analysis.

3.2. Combinatorial effect of fucoidan with zymosan on macrophage activation in RAW264 cells

To evaluate the synergistic effect between fucoidan and zymosan on immune response, RAW264 cells were co-treated with fucoidan and zymosan. As shown in Fig. 2-3, the treatment with zymosan alone markedly elevated the production of NO and TNF-α in a dose-dependent manner between 125 and 500 ng/mL (open column), indicating that β-glucan exerted the activation of macrophage by oneself.[98] Notably, the production of NO and TNF-α by the co-treatment with fucoidan and zymosan together was much higher as compared to the treatment of fucoidan alone (closed column), suggesting that intracellular signals stimulated by fucoidan and β-glucan were intertwined with each other to enhance immune activation.[14,48] On the other hand, treatment with HKLM, LPS, and FSL-1 (ligand for TLR2, TLR4, and TLR6/2, respectively) also showed significant macrophage activation activity in RAW264 cells without any cytotoxic effects (Fig. 2-4, open column), but unlike zymosan, no synergistic effect with fucoidan was observed (Fig. 2-4, closed column).

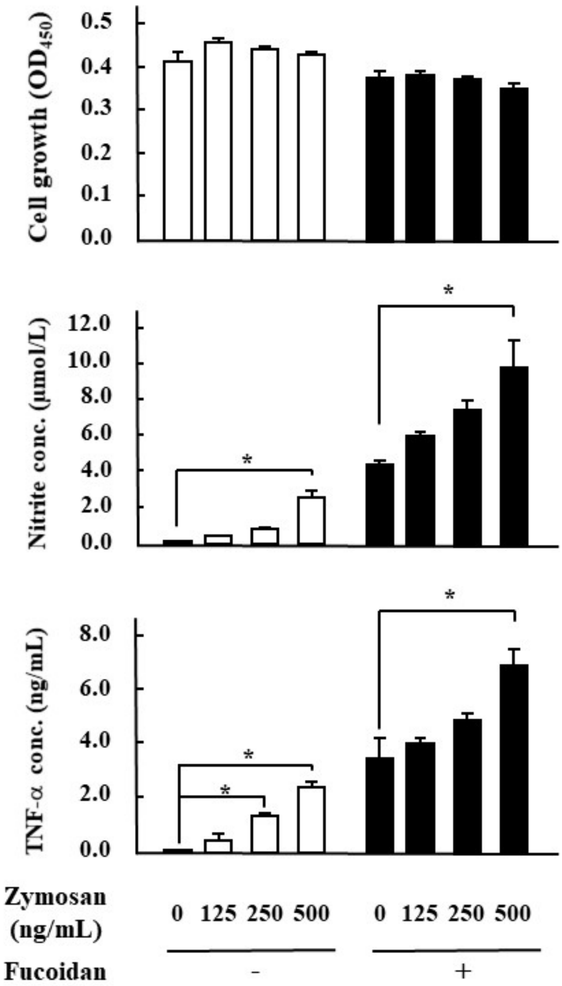

Fig. 2-3. Synergistic effect of fucoidan and zymosan treatment on the macrophage-stimulation activity.

RAW264 cells were cultured in the absence (open column) or presence of 10 μg/mL (closed column) fucoidan with zymosan (0–500 ng/mL). Data were shown as the mean ± SD. Each of the experimental values within each group (fucoidan treated or non-treated groups) was compared to that of the control (non-zymosan-treated). Unpaired Student's *t*-test was used for the evaluation of statistical difference. Asterisk (*) mark on column indicates the significant difference compared to each control (p<0.05, n=3–4).

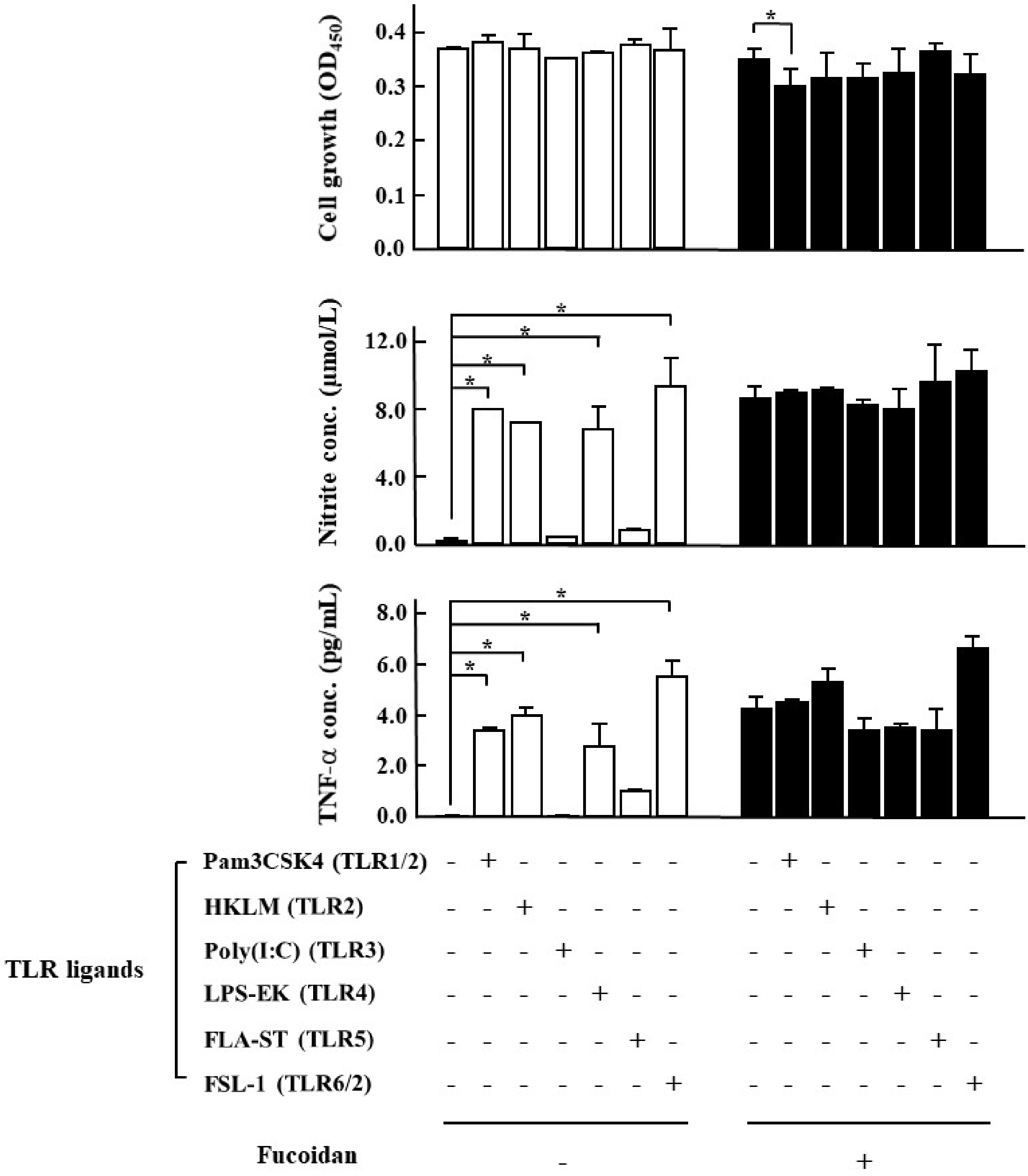

Fig. 2-4. Immune-stimulation activity of fucoidan in co-treatment with ligands for TLRs.

RAW264 cells were treated with each TLR ligands in the absence (open column) or presence (closed column) of 10 μg/mL fucoidan. Pam3CSK4, ligand for TLR1/2; HKLM, ligand for TLR2; Poly(I:C), ligand for TLR3; LPS-EK, ligand for TLR4; FLA-ST, ligand for TLR5; and FSL-1, ligand for TLR6/2 were prepared as stated in the section of Materials and Methods. Data were shown as the mean ± SD. Each of the experimental values within each group (fucoidan treated or non-treated groups) was compared to that of the control (non-TLR ligands-treated). Unpaired Student's *t*-test was used for the evaluation of statistical difference. Asterisk (*) mark on column indicates the significant difference when compared to each control (p<0.05, n=3–4).

3.3. Involvement of lipid rafts of RAW264 cells in the synergistic immune-stimulation activity of fucoidan with zymosan

Lipid rafts are specialized regions in the plasma membrane, in which PRRs such as TLRs and dectin-1 are recruited in the process of the activation of macrophage through the recognition of PAMPs.[99,100] Thereby, to explore that the receptors involved in the synergistic immune-stimulation activity between fucoidan and zymosan are associated with lipid rafts, lipid rafts in RAW264 cell membrane were eliminated by cholesterol depletion induced by the pretreatment with methyl β-cyclodextrin prior to sample treatment.[95] As shown in Fig. 2-5, the RAW264 cells NO production caused by zymosan treatment was offset by methyl β-cyclodextrin treatment, resulting in attenuating the synergistic effect between fucoidan and zymosan. These results suggested that receptors for zymosan were located at lipid rafts during signal transduction.[99,101] However, the NO production in fucoidan-treated RAW264 cells was not obstructed by removing lipid rafts in cell membrane, suggesting that receptors for fucoidan might not be associated with lipid rafts, or fucoidan could target multiple receptors, thus participating in stimulatory or inhibitory cell signaling.[102]

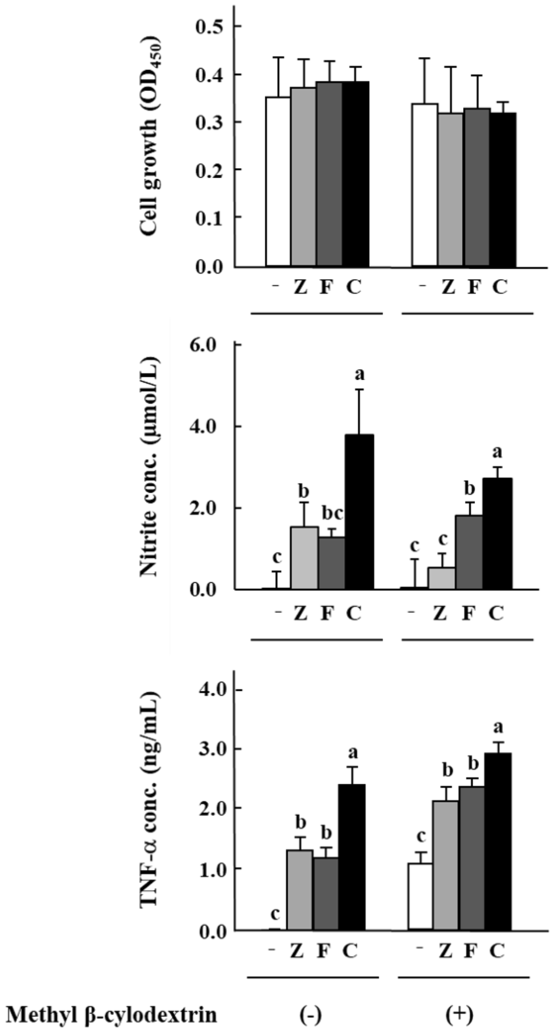

Fig. 2-5. Effects of lipid rafts disruption on the synergistic immune-stimulation activity of fucoidan with zymosan.

RAW264 cells were pretreated with 5 mmol/L methyl β-cyclodextrin to disrupt lipid rafts prior to sample treatment (500 ng/mL zymosan (Z), 10 µg/mL fucoidan (F) or co-treatment (C)). Data were shown as the mean ± SD. Statistical differences between experimental values within each group (methyl β-cyclodextrin treated or non-treated groups) were evaluated by Tukey-Kramer test. Different small letters on column indicate significant differences (p<0.05, n=3–4).

3.4. Elucidation of zymosan components in the synergistic immune-stimulation by combinatorial treatment of fucoidan and zymosan in RAW264 cells

It has been reported that zymosan can be a ligand for dectin-1 as well as TLR2.[94] However, given that no synergistic effect between fucoidan and TLR2 ligand (HKLM) was observed (Fig. 2-4), dectin-1 was assumed to contribute to the synergistic macrophage-activation activity by co-treatment with fucoidan and zymosan. To clarify the participation of dectin-1 on the synergistic effect, depleted-zymosan, which activates dectin-1 without stimulating TLR2,[94] was used. As a result, similar to zymosan, depleted-zymosan cooperated with fucoidan to enhance the production of NO and TNF-α in RAW264 cells (Fig. 2-6). In contrast, the synergistic effect was attenuated in the dectin-1 knockdown RAW264 cells transfected with siRNA (Fig. 2-7). These results clearly indicate that dectin-1 rather than TLR2 may be involved in the synergistic macrophage-stimulation effect between fucoidan and zymosan.

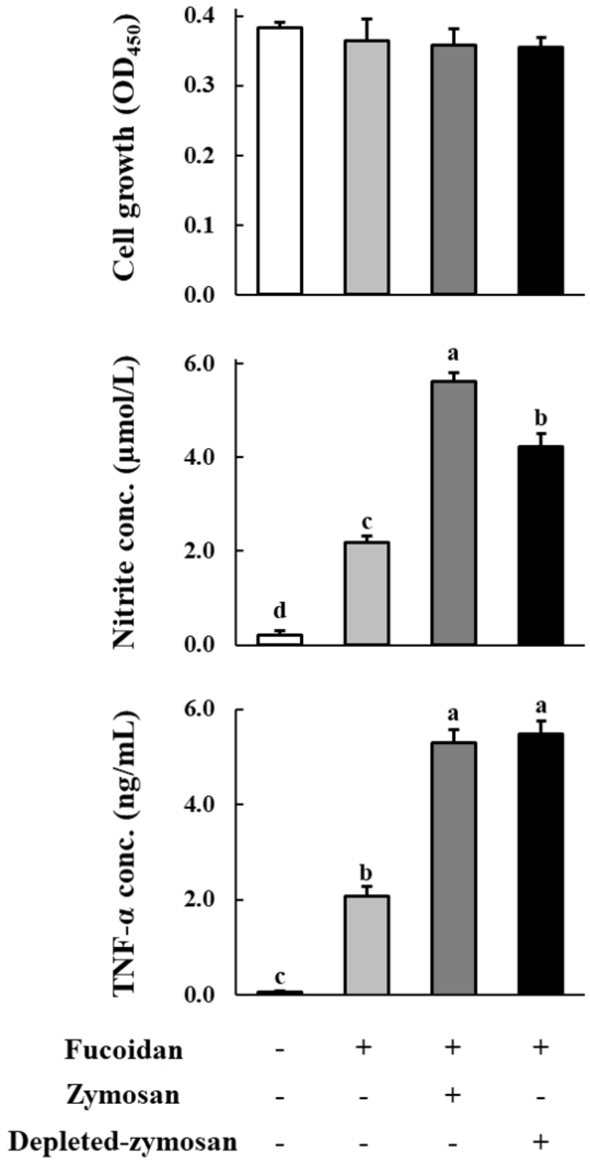

Fig. 2-6. Comparison of immune-stimulation activity between zymosan and depleted-zymosan in co-operative action with fucoidan.

RAW264 cells were treated with 500 ng/mL zymosan or 100 ng/mL depleted-zymosan in the absence or presence of 10 μg/mL fucoidan. Data were shown as the mean ± SD. Tukey-Kramer test was used for the evaluation of statistical differences. Different small letters on column indicate significant differences at $p<0.05$ (n=3–4).

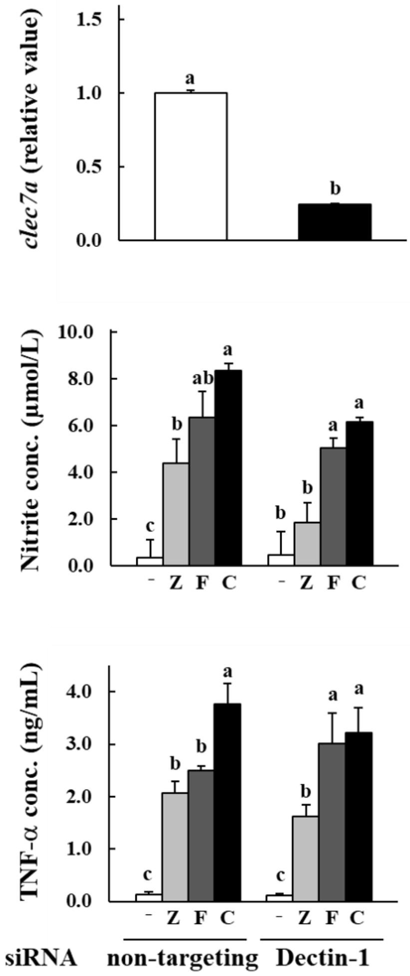

Fig. 2-7. Dectin-1-related macrophage-stimulation activity of fucoidan with zymosan.

RAW264 cells transfected with non-targeting (knockdown control) or dectin-1 siRNA were treated with 500 ng/mL zymosan (Z), 10 µg/mL fucoidan (F) or the co-treatment (C). Data were shown as the mean ± SD. Tukey-Kramer test was used for evaluating statistical differences between expression levels of *clec7a*. Experimental values of nitric oxide and tumor necrosis factor (TNF)-α productions within each group (knockdown control or dectin-1 knockdown groups) were compared by Tukey-Kramer test. Different small letters on column indicates significant differences (p<0.05, n=3–4).

4. Summary

In conclusion, **Chapter II** demonstrates that *C. okamuranus* fucoidan exhibited the immune-stimulation activity by interacting with some cell surface receptors probably including PRRs expressed on plasma membrane of RAW264 cells. In addition, the fucoidan cooperated with zymosan to enhance immune function through activating macrophage. The synergistic effect is likely related to the cell signaling occurring from the activation of PRRs (such as dectin-1) arranged to lipid rafts.

Chapter III

Ligand-assisted nuclear magnetic resonance (NMR) spectrometry assay for sulfate content in sulfated polysaccharides

1. Introduction

Sulfated polysaccharides are a main constituent of cell wall of seaweeds. Sulfate groups in sulfated polysaccharides are considered as a key structural factor in exhibiting physiological activities, such as anti-cancer, anti-thrombin, and anti-tumor effects.[24-26,31,102,103] For example, Sun *et al*.[51] reported that RAW264 cells treated by sulfated polysaccharide fraction derived from *Caulerpa lentillifera* containing ca. 22 wt% of sulfate group exhibited much higher immune-stimulation activity when compared to a fraction with ca. 12 wt% of sulfate group. Therefore, an appropriate sulfate assay is strongly required to assess biological functions of sulfated polysaccharides.

A convenient assay for the determination of sulfate content in sulfated polysaccharides is based on the precipitation reaction between barium ions and inorganic sulfates liberated by acid hydrolysis.[29,50-52,54,55] Considering the structural feature of sulfate group of sulfated polysaccharides for bioactivity, structural change in polysaccharides during extraction and purification processes should be avoided.[56] However, since the conventional barium assay requires substantially intensive extraction and purification processes, sulfate group in polysaccharides may be released, resulting in a poor reproducibility.[55] Therefore, a further extensive assay for sulfate content in polysaccharides without tedious preparation steps is required.[54-56]

Since NMR spectroscopy is a non-destructive analytical method, qNMR assay has been applied to determine analytes in mixtures such as foods[67-72] and pharmaceutical products.[63,64] To conduct qNMR assay, a well-resolved ^{1}H NMR signal of interests is indispensable. In saccharide assay, anomeric C-1 proton signal is generally targeted.[69,70,78] For example, anomeric C-1 proton signal in glucose was used for the estimation of glucose content in commercial fruit beverages[67] and glucan content in commercially available dietary supplements.[70] However, due to the narrow variance of ^{1}H NMR signals for saccharides, it is extremely hard to obtain a distinct target proton signal including anomeric C-1 proton in mixture.[68,69,78] In sulfated saccharide assay, especially, because of a substituent effect of sulfate group, proton signal at the sulfate group position is shifted to down-field (0.3–0.6 ppm). This shift makes harder to gain well-resolved targeted anomeric C-1 proton signal.[78,104]

In the present study, an NMR titration method was applied for evaluating the sulfate content in sulfated polysaccharides by observing δ values of a ligand showing a 1:1 binding stoichiometry with the sulfate group in sulfated polysaccharides. In the 1:1 binding system, a constant δ value of cationic ligand target proton is observed when a molar concentration of ligand is lower than that of counter anion, whereas the δ value of target proton is shifted when the molar concentration of ligand is higher than that of anion. The NMR titration technique tracks a behavior of ligand δ in the presence of anion to determine a desirable artificial receptor for a certain anion. For example, Jin *et al*.[84] found that a squaramide-based tripodal receptor selectively bound to SO_4^{2-} with a high binding affinity (K of $10^{4.9}$ L/mol) by conducting NMR titration. Other literatures suggested triodal urea, thiourea, indole, or guanidinium groups based receptors showed the high binding affinity with sulfate anion (K>10^4 L/mol).[81-83,105] Therefore, in this study, we firstly screened various candidates to select an appropriate ligand molecule, showing the 1:1 binding stoichiometry with sulfate group in saccharides. Secondly, the application of the proposed ligand-assisted ^{1}H NMR assay for the estimation of sulfate content in sulfated saccharides was evaluated. The sulfate saccharides used in this study were commercially available mono- to tetrasaccharides with defined sulfated content (Fig. 3-1). Lastly, we applied the novel assay to estimate sulfate content in polysaccharides, including the commercially available *F. vesiculosus*-derived fucoidan (Fig. 3-1) and crude polysaccharides extracted from various seaweeds (Table 3-1).

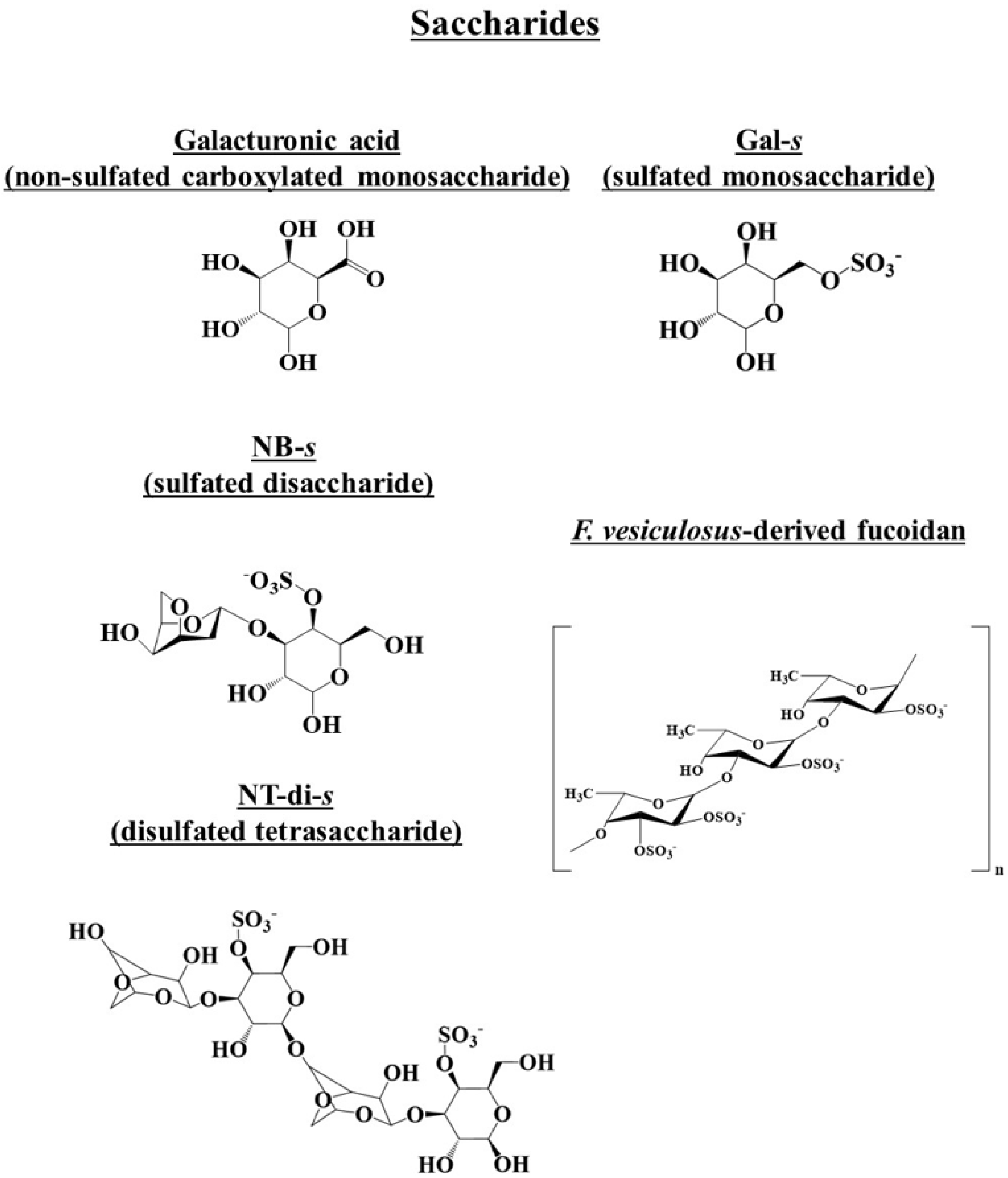

Fig. 3-1. Chemical structure of saccharides used in this study.

Abbreviation of saccharides was used as follow; Gal-*s*, galactose-6-*O*-sulfate; NB-*s*, neocarrabiose-4-*O*-sulfate; and NT-di-*s*, neocarratetraose-41,3-di-*O*-sulfate.

Table 3-1. Commercially available seaweeds used in this study.

Seaweed		Harvest region
Common name	Scientific name	
Aosa-Nori	*Monostroma nitidum*	Aichi
Nori	*Porphyra yezoensis*	Shizuoka
Akamoku	*Sargassum horneri*	Aichi
		Miyagi
		Mie
		Nagasaki
Gagome-Kombu	*Kjellmaniella crassifolia*	Sapporo
Ishi-Mozuku	*Sphaerotrichia firma*	Aomori Niigata
Kombu	*Saccharina japonica*	Iwate
Mekabu	Sporophyll of *Undaria pinnatifida*	Miyagi Shimane
Okinawa-Mozuku	*Cladosiphon okamuranus*	Ishigaki Island Kume Island Miyako Island Tsuken Island
Wakame	*Undaria pinnatifida*	Iwate Miyagi Nagasaki Tokushima

2. Materials and Methods

2.1. Materials

L-ascorbic acid, D-(+)-Galactose (Gal), L-arginine, barium chloride dihydrate, 1-ethyl-3-(3-dimethylaminopropyl) carbodiimide (EDC), glycine, imidazole, $NaBH_4$, and Na_2SO_4 were purchased from Nacalai Tesque Inc. (Kyoto, Japan). 3β-galactobiose (β-Gal-[1→3]-Gal) (di-Gal), 3α-4β-3α-galactotetraose (α-Gal-[1→3]-β-Gal-[1→4]-α-Gal-[1→3]-Gal) (tetra-Gal), galactose-6-*O*-sulfate (Gal-*s*), neocarrabiose-4-*O*-sulfate (NB-*s*), and neocarratetraose-41,3-di-*O*-sulfate (NT-di-*s*) were products from Dextra Laboratories Ltd. (Shinfield, UK); all sulfated chemicals were in the form of sodium salts. *F. vesiculosus*-derived fucoidan was purchased from Sigma-Aldrich Co. (≥ 95% pure, Cat. No. F8190, St. Louis, MO, USA). D-(+)-Galacturonic acid monohydrate, piperazine hexahydrate, and 3-(trimethylsilyl) propionic-2,2,3,3-d_4 acid (TSP-d_4) were purchased from Wako Pure Chemical Co. (Osaka, Japan). Deuterium oxide (D_2O, 99.8 atom% D), 1-(2-pyrimidinyl) piperazine, and sodium rhodizonate were gained from Kanto Chemical Co. Inc. (Tokyo, Japan). All pickled seaweeds (one green, one red, and seven brown seaweeds) listed below were harvested at different regions were obtained from local Japanese markets (Table 3-1). The green and red seaweeds were Aosa-Nori (*Monostroma nitidum*) and Nori (*Porphyra yezoensis*), respectively. The brown seaweeds were as follows: Akamoku (*Sargassum horneri*), Gagome-Kombu (*Kjellmaniella crassifolia*), Ishi-Mozuku (*Sphaerotrichia firma*), Kombu (*Saccharina japonica*), Mekabu (Sporophyll of *U. pinnatifida*), Okinawa-Mozuku (*C. okamuranus*), and Wakame (*U. pinnatifida*).

2.2. ^{1}H and ^{13}C NMR measurements

One-dimensional ^{1}H and ^{13}C NMR spectroscopies were performed at 25°C using an ECS-400 spectrometer (JEOL, Tokyo, Japan). For acquiring ^{1}H NMR spectra, a single pulse sequence was performed with the following parameters: 2.18 s for acquisition time; data acquisition points of 16,384; 5 s for relaxation delay; and spinning at 15 Hz. In addition, a suitable scan number (8–512) was employed to obtain ^{1}H NMR signals of ligands with higher signal to noise ratio (> 3:1).[106] For obtaining ^{13}C NMR spectra, a single pulse sequence was conducted with the following parameters: 2.18 s for acquisition time; data acquisition points of 32,768; scan number of 20,000–30,000; 2 s for relaxation delay; and spinning at 15 Hz. TSP-d_4 used as an external reference (0.00 ppm) was not mixed with the sample dissolved in D_2O for avoiding any interference of TSP-d_4 carboxy group on the interaction between ligand molecule and sulfate group in sulfated saccharides. Instead, prior to measurement, a 3.5 mm-stem coaxial insert NMR tube (Nihon Seimitsu Scientific Co., Tokyo, Japan) containing TSP-d_4 dissolved in D_2O was inserted into a 5 mm-NMR tube (Nihon Seimitsu Scientific Co.) filled with 400 μL of sample dissolved in D_2O.

2.3. Preparation of ligand-sulfated saccharide solution

To avoid the interference of cation such as Na^+ on the interaction between ligand molecule and sulfate group in saccharides, desalting was performed with TOYO-PAK

IC-SP M cartridge (TOSOH Co., Tokyo, Japan) prior to the preparation of sample solution. The filtrate was lyophilized, weighed, and dissolved in D_2O. All ligand candidates were also dissolved in D_2O and mixed with the saccharide solution to be the molar ratios of 0.2:1 to 3:1. The final concentration of saccharide solution was fixed to be 8.3 mmol/L for all tested sample. Saccharides containing no sulfate group (e.g., Gal, di-Gal, and tetra-Gal) were used as negative controls.

To investigate the unanticipated affinity of carboxy group to ligand molecule, which may possibly induce $\Delta\delta$ of ligand, galacturonic acid, a monosaccharide bearing carboxy group instead of sulfate group was used (Fig. 3-1). A methyl-α-D-galacturonate (or methyl galacturonate) was prepared by following the protocol reported by Jansen and Jang[107] with minor modifications. In brief, 1 g of galacturonic acid dissolved in 31 mL of 25 mmol/L HCl/methanol was incubated for three days at 4°C. The solution was then neutralized with KOH/MeOH and evaporated under N_2 atmosphere. The residue was diluted with de-ionized water and employed to TOYO-PAK DEAE and TOYO-PAK IC-SP M cartridges (TOSOH Co.) for removing the residual galacturonic acid and cations, respectively. The filtrated methyl galacturonate solution was freeze-dried and re-dissolved in D_2O for subsequent ^{1}H NMR measurement.

2.4. Extraction of sulfated polysaccharides from seaweeds

Pickled seaweeds were washed with tap water to desalt and dried by lyophilization. The dried sample (20–25 g) was soaked in 300 mL of boiling-water for 1 h to obtain crude polysaccharide fraction. The supernatant was then pooled after centrifugation

(10,810 *g*; 20 min; 10°C). The extraction procedure was repeated three times. The pooled extract was concentrated by rotary evaporation. To eliminate interference with carboxy group, carboxy group rich polysaccharide including alginate was removed by precipitation reaction with the continuous addition of 50 wt% $CaCl_2$ until no more precipitate occurred. Alginate-free supernatant was collected after centrifugation (13,980 *g*; 30 min; 10°C), and the solution was dialyzed (membrane MW cut off: 12,000; Nacalai Tesque) against de-ionized water for 72 h or more while changing the dialysis water once every 12 h. The dialysate was concentrated, dried, and used as crude polysaccharide.

2.5. Reduction of carboxy group in polysaccharides

To remove residual carboxy group in crude polysaccharides, a chemical reduction procedure was performed with EDC and $NaBH_4$,[30] prior to ^{1}H NMR measurement. In brief, 100 mg of EDC was gradually added to 5 mL of crude polysaccharide solution (20 mg/mL) dissolved in de-ionized water. The pH of solution was adjusted to 4.75–5.0 using 0.1 mol/L HCl with continuous stirring for 2 h. $NaBH_4$ (500 mg) was then added while stirring, and the pH was set to be 7.0 with 6 mol/L HCl for 1 h. To prevent foaming, a few drops of ethanol (EtOH) were added. The reactant was dialyzed (membrane MW cut off: 12,000; Nacalai Tesque) against de-ionized water for 48 h, followed by desalting with TOYO-PAK IC-SP M cartridge (TOSOH Co). The filtrate was dried, weighed, and dissolved in D_2O for subsequent NMR measurement. To confirm the chemical reduction of carboxy group to hydroxymethyl group in crude polysaccharide, the appearance of

^{13}C NMR signal at 59.0 ppm (hydroxymethyl group) and the disappearance of ^{13}C NMR signal at 178.1 ppm were obtained.[30,78] On the other hand, as commercially available *F. vesiculosus*-derived fucoidan rarely contains carboxy group (Fig. 3-1),[108] the chemical reduction process was not performed prior to ^{1}H NMR measurement.

2.6. Ligand-assisted ^{1}H NMR assay for sulfate content in *Fucus vesiculosus*-derived fucoidan and crude sulfated polysaccharides

To evaluate the sulfate content of commercially available fucoidan derived from *F. vesiculosus* and various seaweeds-derived crude polysaccharides by the ligand-assisted ^{1}H NMR assay, imidazole dissolved in D_2O was mixed with fucoidan or reduced crude polysaccharides dissolved in D_2O to be the concentration of 0.1–6.25 mmol-imidazole/g of sample; the concentration of polysaccharides was fixed to be 0.08 mg/mL. δ values of imidazole target protons were observed and plotted against imidazole concentration. To investigate the sensitivity of the present ^{1}H NMR assay, Limit of Detection (LOD) for imidazole target protons at the scanning number of 512 was computed. To confirm the accuracy of the sulfate content estimated by the ligand-assisted ^{1}H NMR assay, the estimated sulfate content values were compared to those obtained by a conventional barium-rhodizonate assay.[109] To estimate sulfate content by the barium-rhodizonate assay, fucoidan and native crude polysaccharides were subjected to acid hydrolysis (105°C for 2 h). The aliquot (0.5 mL) was then mixed with 2.0 mL of EtOH, 1.0 mL of barium buffer (containing 0.2 mmol/L $BaCl_2$; 1.6 mmol/L $NaHCO_3$; 0.2 mol/L acetic acid; and 80% EtOH), and 1.5 mL of rhodizonate reagent (containing 50 μg/mL sodium rhodizonate; 1 mg/mL L-ascorbic acid; and 80% EtOH), followed by an incubation for 10 min at room temperature in the dark. The absorbance of reactant was measured at 520 nm and the standard curve (Na_2SO_4 as standard) reflected the range of 0–24 μg/mL of sulfate.

2.7. Statistical analysis

Because δ value is invariable under fixed NMR conditions, no replicate ^{1}H NMR measurement was performed in this study. The conventional barium-rhodizonate assay was performed in triplicate for each sample. The estimated sulfate content values from the barium-rhodizonate assay are shown as the mean ± standard deviation (SD). Statistical difference was evaluated by unpaired Student's *t*-test.

3. Results and Discussion

3.1. Screening of ligands for ^{1}H NMR-guided sulfated saccharides assay

In this study, an appropriate ligand, which shows cationic properties allowing to form a 1:1 stoichiometric complex with the sulfate group in sulfated polysaccharides, was required. Since it has been reported that compounds bearing ammonium/guanidinium[82-84] and azacyclic group [85-88] can bind to sulfate anion with higher binding affinity, L-arginine, glycine, imidazole, piperazine, and 1-(2-pyrimidinyl) piperazine were used as typical ligand candidates in the present ligand-assisted ^{1}H NMR assay (Fig. 3-2).

Ligand candidates

L-Arginine

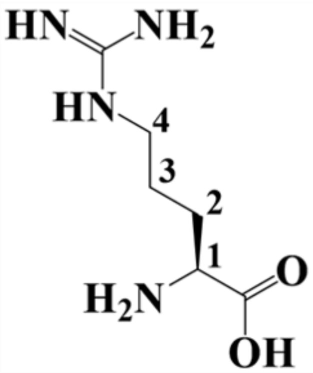

Imidazole

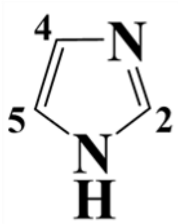

Glycine

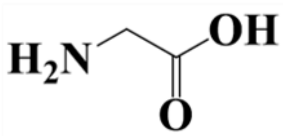

Piperazine

1-(2-Pyrimidinyl) piperazine

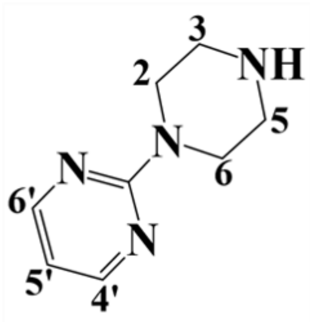

Fig. 3-2 Chemical structure of ligand candidates used in this study.

As shown in Fig. 3-3, $\Delta\delta$ of ^{1}H NMR signal for candidates in the presence or absence of an equivalent amount of monosulfated disaccharide (NB-*s*) was observed. Among the candidates, δ values of glycine, piperazine, and imidazole were remarkably moved to down-field ($\Delta\delta \geq 0.15$ppm), whereas no or relatively smaller shifts were observed for L-arginine and 1-(2-pyrimidinyl) piperazine. Despite the outstanding $\Delta\delta$ values for glycine (0.15 ppm) and piperazine (0.28 ppm) by the complexing with NB-*s*, their proton signals were found at around 3.5 ppm, which may overlap with those of the saccharides.[69,70,78] For L-arginine, after the addition of NB-*s*, the typical protons were not clearly distinguished. In contrast, upon the addition of NB-*s* to imidazole, imidazole protons showed outstanding $\Delta\delta$ (H2: 0.79 ppm; H4,5: 0.29 ppm), and were observed at the δ region (7.15–8.59 ppm), clearly separated from the saccharide region (3.5–5.5 ppm).[70,78] This result was in line with that of literature, stating that the δ value of H2 of imidazolium ring in xylene-based imidazolium receptor was drastically shifted to a lower magnetic field in the presence of HSO_4^-.[88] However, due to much lower intensity of H2 signal compared to H4,5 signal, the H4,5 signal was selected for further experiments to explore the ligand activity of imidazole against sulfated saccharides as a target proton.

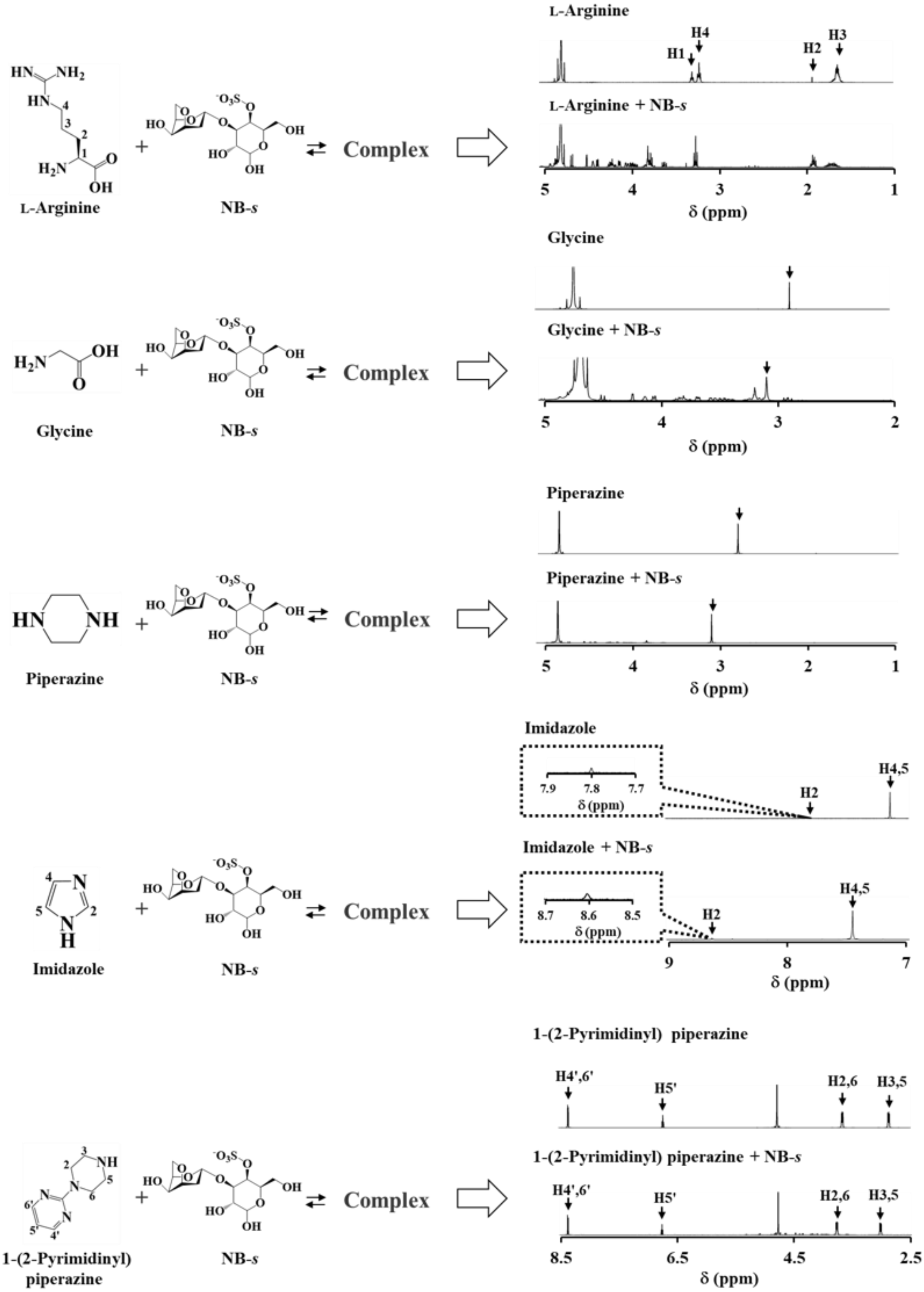

Fig. 3-3 Comparison of the chemical shift (δ) values for protons of ligand candidates in the presence and absence of an equivalent amount of sulfated saccharide.

A neocarrabiose-4-*O*-sulfate (NB-*s*) was used as a representative sulfated saccharide. The concentration of tested candidates and NB-*s* was 8.3 mmol/L. The detailed conditions of ^{1}H NMR measurement were stated in the section of Materials and Methods. Arrow indicates target protons of candidates.

3.2. Stoichiometric complex formation of imidazole with sulfated saccharides

To understand a stoichiometric complex formation between imidazole and sulfate group in sulfated saccharides, δ values of imidazole target protons (H4,5) at different molar ratios of imidazole to NB-*s* (0.2:1 to 3:1) were measured. To exclude the effect of an incremental saccharide viscosity on imidazole ^{1}H NMR signals,[64,110] the concentration of NB-*s* in all tested samples was fixed to be 8.3 mmol/L.

As shown in Fig. 3-4, the presence of NB-*s* induced Δδ of imidazole H4,5 toward lower magnetic field, and the δ value was constant at lower molar ratios than 1:1, indicating all imidazole molecules were likely to be saturated.[82] However, at higher molar ratios than 1:1, due to an increase of free imidazole molecules, the δ value of imidazole H4,5 gradually shifted to higher magnetic field. These results demonstrated that imidazole molecule ionically form the 1:1 stoichiometric complex with sulfate group in NB-*s*. This is in agreement with the previous result found in the literature that described the constant δ value of imidazolium H2 was observed when a molar ratio of xylene-based symmetric receptor to HSO_4^- was below 1:1.[88] In addition, a plot based on the observed δ values of imidazole H4,5 against the different molar ratios of imidazole to NB-*s* (Fig. 3-5) can allow to estimate sulfate content in sulfated saccharides. When observed δ values of imidazole were schematized against molar concentrations of imidazole, by the 1:1 binding stoichiometry between imidazole and sulfate group in saccharides, molar concentration of imidazole at the inflection point of the plot may correspond to that of sulfate content in sulfated saccharides.

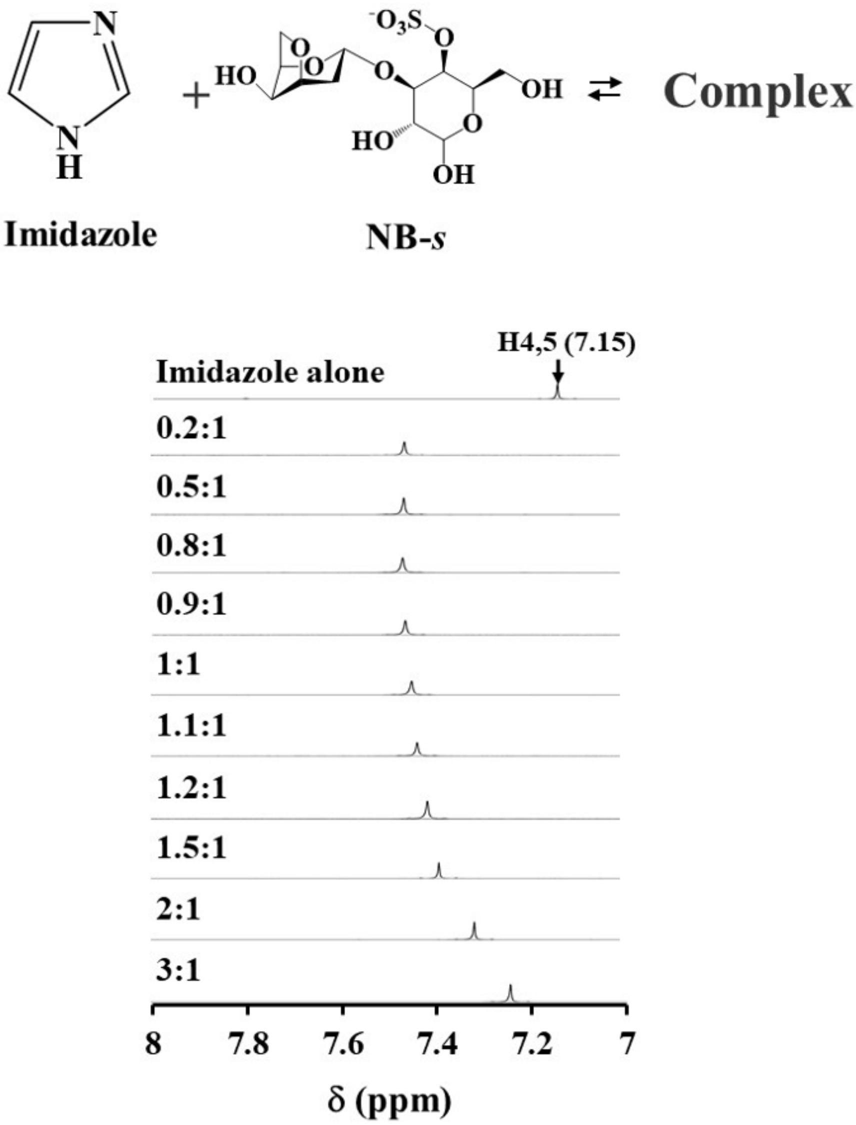

Fig. 3-4. Change in chemical shift ($\Delta\delta$) of imidazole target proton (H4,5) at different molar ratios of imidazole to the sulfated saccharide, NB-*s*.

Neocarrabiose-4-*O*-sulfate (NB-*s*) was used as sulfated saccharide, and the concentration of NB-*s* was fixed to 8.3 mmol/L. Different concentration of imidazole was mixed with NB-*s* solution to be the concentration of 8.3–25 mmol/L (molar ratios of 0.2:1–3:1). The detail conditions of ^{1}H NMR measurement were stated in the section of Materials and Methods.

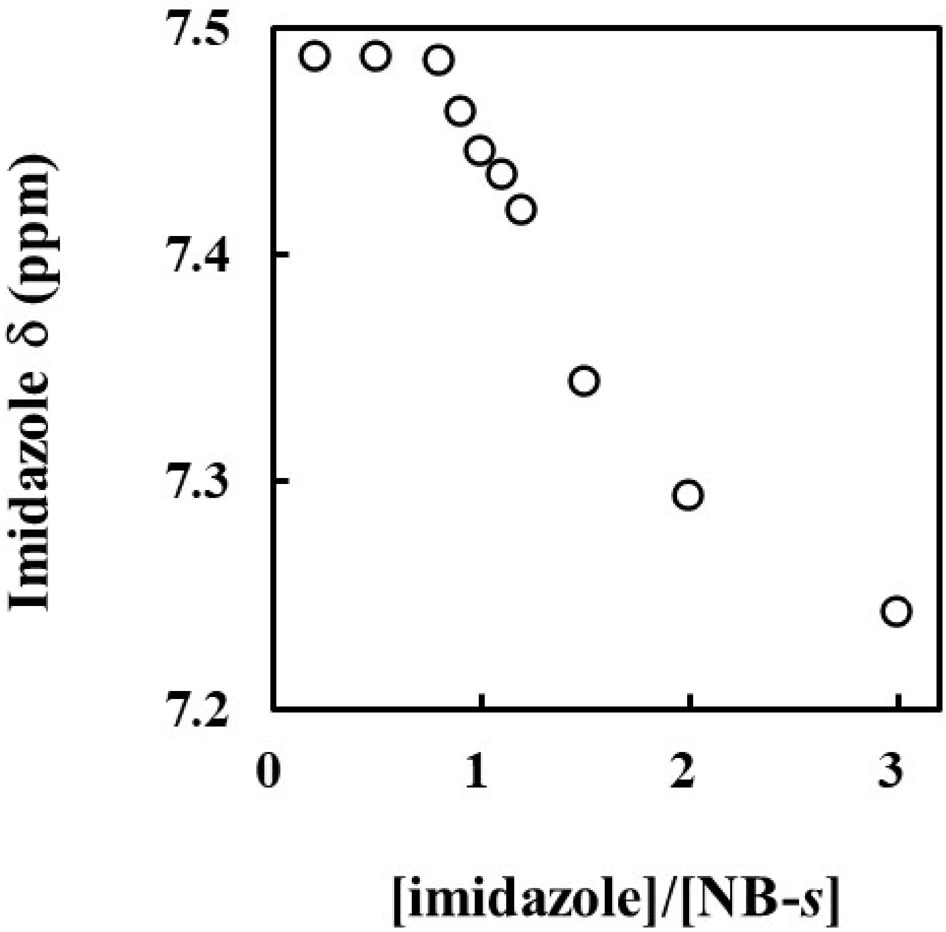

Fig. 3-5. A plot of chemical shift (δ) of imidazole target proton (H4,5) *vs.* molar ratio of imidazole to sulfated saccharide, NB-*s*.

δ values of imidazole were obtained from the result of Fig. 3-4. Neocarrabiose-4-*O*-sulfate (NB-*s*) was used as sulfated saccharide, and the concentration of NB-*s* was fixed at 8.3 mmol/L.

However, to apply imidazole as a ligand for estimating sulfate content in various polysaccharides, the effect of the number of sulfate group in monomeric unit and/or structure and molecular size of sulfated saccharides on the stoichiometric complex formation between imidazole molecule and sulfate group in saccharides should be explored. Therefore, in this study, monosulfated mono- and di-saccharides (Gal-*s* and NB-*s*, respectively) and disulfated tetrasaccharide (NT-di-*s*) were used. As negative controls, their corresponding saccharides bearing no sulfate group; mono-, di-, and tetrasaccharides (Gal, di-Gal, and tetra-Gal, respectively) were used. To ensure that the molar ratio of imidazole to sulfate group in sulfated saccharides was set to 1:1, all tested samples contained the same concentration (8.3 mmol/L) of saccharide and imidazole; the tested sample for disulfated saccharide, NT-di-*s*, exceptionally contained 8.3 mmol/L NT-di-*s* and 16.7mmol/L imidazole.

As shown in Fig. 3-6, ^{1}H NMR signal of the imidazole H4,5 (7.15 ppm) was not shifted by the addition of non-sulfated saccharides, whereas a remarkable down-field shift was observed by the addition of sulfated saccharides. The same magnitude of δ value of imidazole H4,5 was observed in the presence of each sulfated saccharide together with its corresponding saccharide bearing no sulfate group. These results indicated that an imidazole molecule can selectively bind to a sulfate group in mono- to tetra-saccharides, irrespective to the presence of contaminating neutral saccharides. $\Delta\delta$ values of imidazole H4,5 in the presence of Gal-*s* ($\Delta\delta$ of 0.23 ppm) and NT-di-*s* ($\Delta\delta$ of 0.22 ppm) were smaller than that of NB-*s* ($\Delta\delta$ of 0.29 ppm), indicating that the different substituent positions of sulfate group in saccharides can possibly influence the binding affinity of imidazole with sulfate group in saccharides. To understand the factors involved in the magnitude of $\Delta\delta$ in the presence of sulfated saccharides, K values for imidazole to sulfate group in each saccharide were required. The reported K value of imidazole to sulfate anion in DMSO-d_6 was 350 L/mol,[86] and this value is in the range of sufficient affinity of ligand to anions (80 L/mol for Br^- to > 10^4 L/mol for SO_4^{2-}),[82] suggesting that imidazole, in this study, may behave as a reliable ligand for binding to sulfate group in saccharides in D_2O solution.

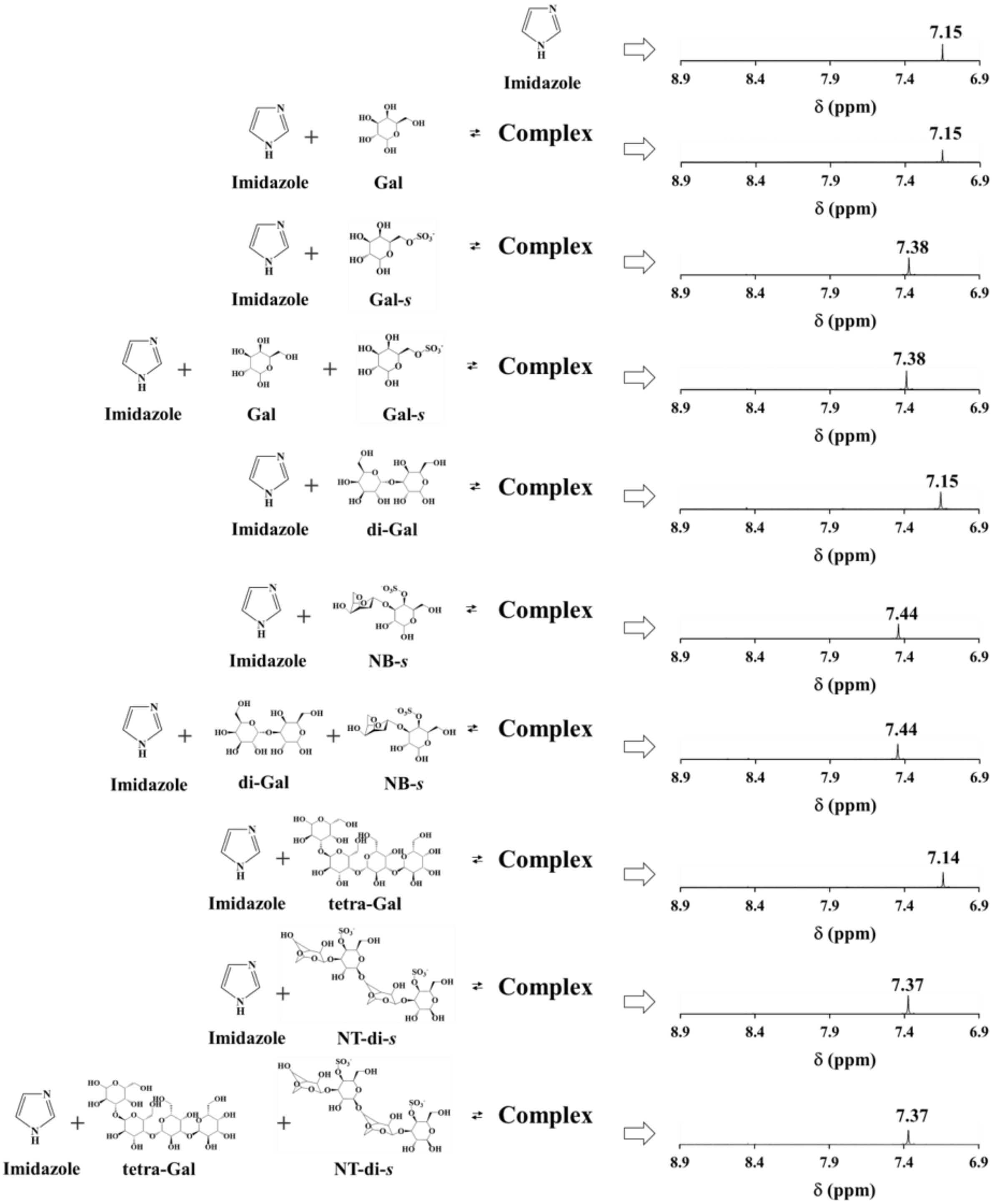

Fig. 3-6. Chemical shift (δ) values of imidazole target protons (H4,5) in the absence or presence of an equivalent amount of non-sulfated and/or sulfated saccharides.

The concentration of all tested sample was 8.3 mmol/L; exceptionally, to set molar ratio of imidazole and sulfate group in neocarratetraose-41,3-di-*O*-sulfate (NT-di-*s*) at 1:1, the concentrations of NT-di-*s* and imidazole were 8.3 and 16.7 mmol/L, respectively. Galactose-6-*O*-sulfate (Gal-*s*), neocarrabiose-4-*O*-sulfate (NB-*s*), and NT-di-*s* were used as sulfated saccharides, and D-(+)-galactose (Gal), 3β-galactobiose (di-Gal), and 3α-4β-3α-galactotetraose (tetra-Gal) bearing no sulfate group were used as their corresponding saccharides. The detailed conditions of ^{1}H NMR measurement were stated in the section of Materials and Methods.

In addition to non-sulfated and sulfated saccharides, carboxylated saccharides including galacturonic and alginic acids[5,103] also occur naturally in seaweeds. It has been reported that carbonate anion formed a complex with imidazolium.[86] Therefore, saccharides bearing carboxy group can possibly disturb the complex formation of imidazole with sulfate group in saccharides, resulting in interfering the estimation of sulfate content in saccharides by the proposed ligand-assisted ^{1}H NMR assay in this study. To apply the ligand-assisted ^{1}H NMR assay for the estimation of sulfate content in natural polysaccharides, thus, the removal of carboxy group in saccharides should be prioritized. As shown in Fig. 3-7, galacturonic acid used as carboxylated saccharide induced a significant $\Delta\delta$ of imidazole H4,5 toward down-field (7.15 to 7.47 ppm), which was similar to the magnitude of $\Delta\delta$ value observed for sulfated saccharides (Fig. 3-6). Considering pK_a value of galacturonic acid (3.24),[111] ionized galacturonic acid allowed to the formation of complex between carboxy group in galacturonic acid and imidazole dissolved in D_2O. In contrast, no $\Delta\delta$ of imidazole H4,5 in the presence of the carboxy group-removed galacturonic acid (methyl galacturonate) was observed. The δ value of imidazole H4,5 in the presence of NB-*s* was matched with that in the presence of both NB-*s* and methyl galacturonate. These results suggested that the removal of carboxy group in saccharide is a reliable and essential pretreatment procedure to guarantee the binding selectivity of imidazole to sulfate group in saccharides for the evaluation of sulfate content in saccharides.

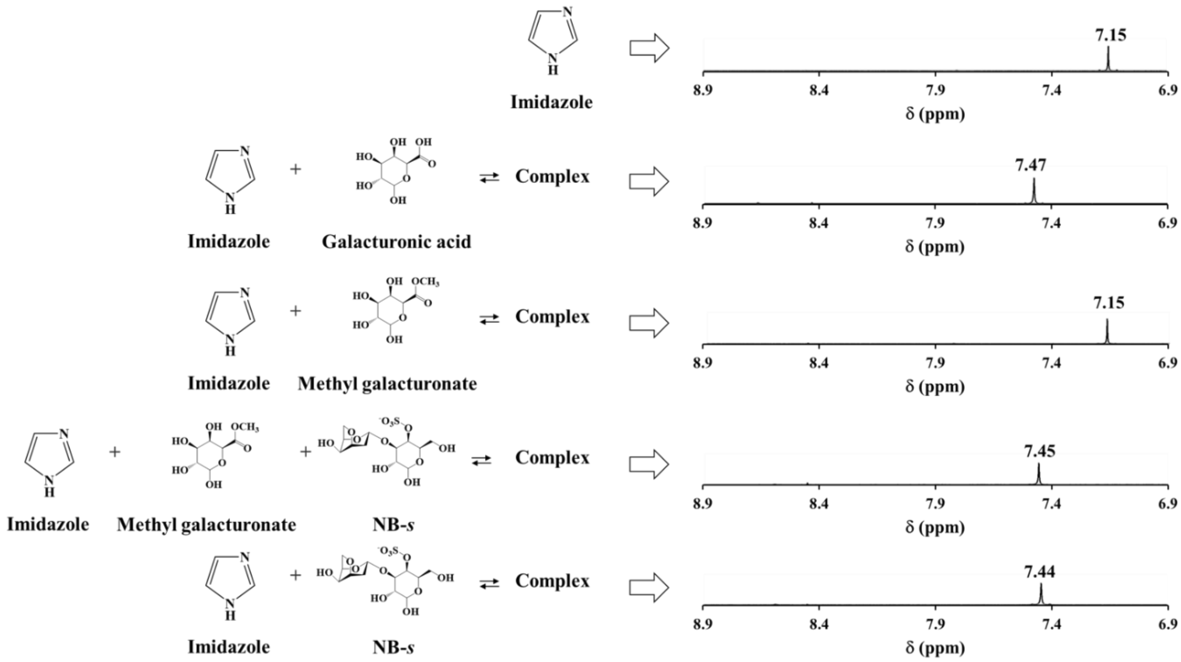

Fig. 3-7. Chemical shift (δ) values of imidazole target protons (H4,5) in the presence or absence of equivalent amount of carboxylated and/or sulfated saccharide.

Galacturonic acid was used as carboxylated saccharide and esterified to methyl galacturonate (methyl-α-D-galacturonate) which was used as decarboxylated saccharide. Esterification experiments were described in the section of Materials and Methods. Neocarrabiose-4-*O*-sulfate (NB-*s*) was used as sulfated saccharide. Final concentration of each saccharide and imidazole was 8.3 mmol/L.

3.3. Sulfate content in *Fucus vesiculosus*-derived fucoidan by ^{1}H NMR measurement

To apply the proposed ligand-assisted ^{1}H NMR assay for sulfate content estimation in purified sulfated polysaccharides, commercially available *F. vesiculosus*-derived fucoidan (Sigma, ≥ 95% pure, Cat. No. F8190) was used. Estimated sulfate content by ^{1}H NMR was compared to that by the conventional barium-rhodizonate method.[109] As shown in Fig. 3-1, because of no carboxy group in *F. vesiculosus*-derived fucoidan,[108] the intact fucoidan without chemical reduction procedure was used as an analyte for ^{1}H NMR measurement. To avoid the effect of fucoidan viscosity on the imidazole H4,5 signal broadening,[64,110] fucoidan concentration was set at 0.08 mg/mL. As shown in Fig. 3-8, constant δ value of imidazole H4,5 (7.480 ppm) was observed up to 2.0 mmol-imidazole/g-fucoidan, whereas at > 2.0 mmol-imidazole/g-fucoidan, the up-field shift of imidazole H4,5 was observed.

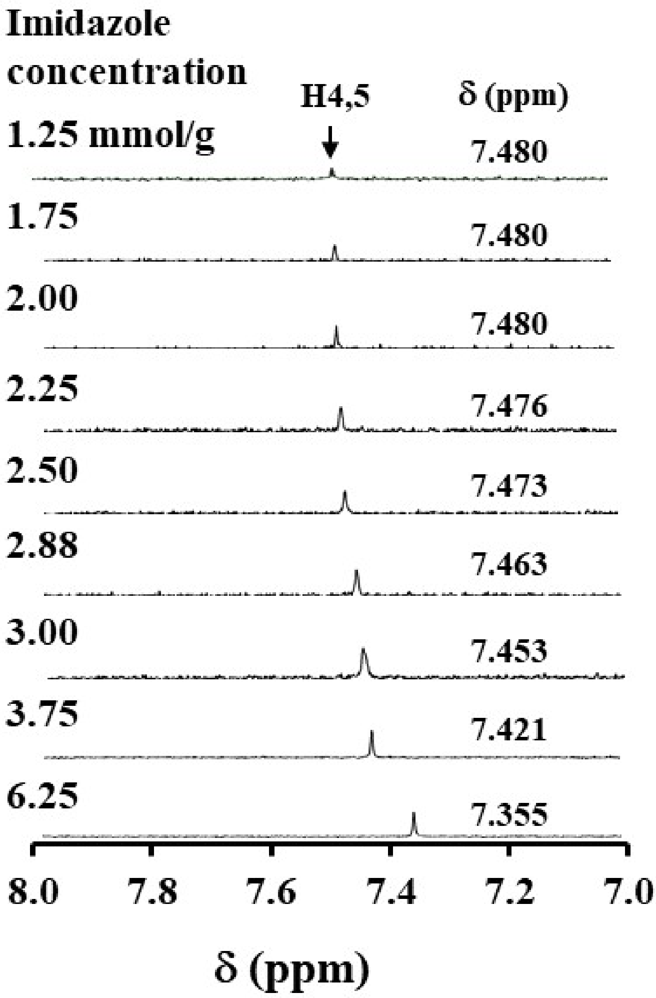

Fig. 3-8. Change in chemical shift (Δδ) of imidazole target proton (H4,5) at different concentrations of imidazole in *Fucus vesiculosus*-derived fucoidan solution.

The concentration of fucoidan was fixed at 0.08 mg/mL. Different concentrations of imidazole were added at 1.25–6.25 mmol-imidazole/g-fucoidan. Conditions of ^{1}H NMR measurement were seen in the section of Materials and Methods.

Notably, as shown in Fig. 3-9, the δ value of imidazole H4,5 against the concentration of imidazole in the range of 2.0–6.25 mmol-imidazole/g-fucoidan showed a good linearity (R^2=0.993). The concentration of imidazole at the inflection point of the plot (observed δ values of imidazole H4,5 *vs.* imidazole concentrations) was estimated to be 2.1 mmol-imidazole/g-fucoidan by the regression equation (Fig. 3-9). This result indicates that the sulfate content in fucoidan was 2.1 mmol-imidazole/g-fucoidan or 20.2 wt%, and the value was matched with that by the barium-rhodizonate assay (20.1±3.2 wt%, *n*=3). In addition, the estimated sulfate content in commercially available *F. vesiculosus* fucoidan by the proposed ligand-assisted ^{1}H NMR assay showed a similar value of 18.2 wt%[112] and 19.0 wt%[58] by a sulfur-elemental analysis.

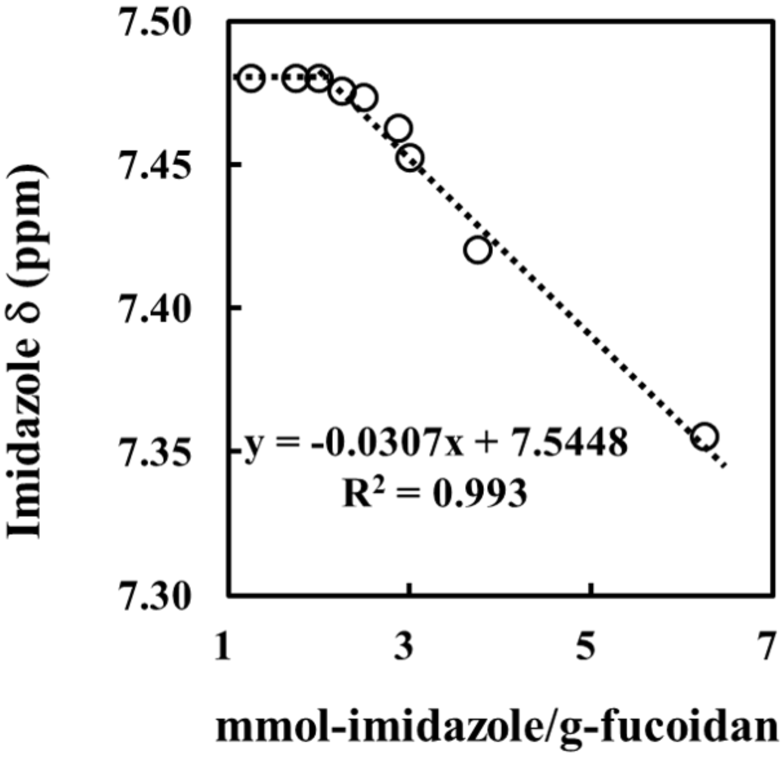

Fig. 3-9. A plot of chemical shift (δ) of imidazole target proton (H4,5) *vs*. concentrations of imidazole in *F. vesiculosus*-derived fucoidan.

δ values of imidazole were obtained from the result of Fig. 3-8. The concentration of fucoidan was fixed at 0.08 mg/mL. Different concentrations of imidazole were added at 1.25–6.25 mmol-imidazole/g-fucoidan.

3.4. Application of ligand-assisted ^{1}H NMR measurement for diverse polysaccharides with sulfate and carboxyl groups

To extensively apply the proposed ligand-assisted ^{1}H NMR assay for seaweed polysaccharides, in this study, a total of twenty crude polysaccharide extracts were prepared with boiling-water from seaweeds spanning nine species and various geographic locations (Table 3-1). To eliminate carboxy group in crude polysaccharides, alginate (highly carboxylated polysaccharide) was removed by precipitation with $CaCl_2$. Subsequently, the residual carboxy group in crude polysaccharides was chemically reduced by using EDC and $NaBH_4$, prior to ^{1}H NMR measurement. Consequently, ^{13}C NMR signal at 178.1 ppm for carboxy group in crude polysaccharides disappeared. Instead, the ^{13}C NMR signal of the reduced form (hydroxymethyl group) newly appeared at 59.0 ppm (Fig. 3-10).[30,78]

To investigate the effect of the chemical reduction treatment on sulfate content, the conventional barium-rhodizonate assay was used for the comparison of the sulfate contents in native (non-reduced) and reduced crude polysaccharides. As a result, there was no significant difference (unpaired Student's t-test, p=0.19) between sulfate content values of native (7.94 ± 0.64 wt%, n=3) and reduced (7.07 ± 0.71 wt%, n=3) crude polysaccharides from Aichi *M. nitidum*. This indicates that the reduced crude polysaccharides may be applicable analyte for estimating sulfate content in crude polysaccharides by the present ligand-assisted ^{1}H NMR assay using imidazole as a ligand.

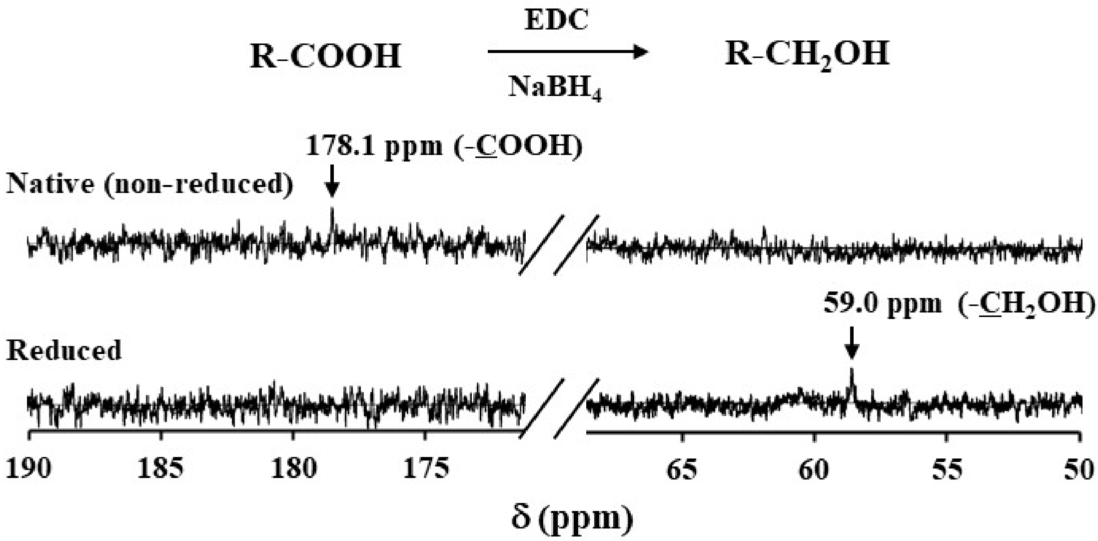

Fig. 3-10. ^{13}C NMR spectra of native (non-reduced) and reduced crude polysaccharides derived from Aichi *Monostroma nitidum*.

The removal of carboxy group in crude polysaccharides by chemical reduction procedure with EDC and $NaBH_4$ was confirmed by observing the disappearance of carboxy group signal at 178.1 ppm and a new appearance of hydroxymethyl group (reduced form) signal at 59.0 ppm in ^{13}C NMR spectra.

3.5. Quantitative evaluation of sulfate content in diverse seaweed polysaccharides by ligand-assisted ^{1}H NMR measurement

For the estimation of sulfate content in diverse crude polysaccharides by an imidazole-assisted ^{1}H NMR assay, reduced crude polysaccharides were prepared as described in section 2.5. To avoid ^{1}H NMR signal broadening due to the synergistic viscosity of polysaccharides,[113] the concentration of reduced crude polysaccharides was fixed at 0.08 mg/mL. Given that LOD for imidazole H4,5 at the scanning number of 512 was 0.011 mmol-imidazole/g-reduced crude polysaccharide, the proposed ^{1}H NMR assay showed sufficient sensitivity to estimate the sulfate content in crude polysaccharides, a mixture of various seaweed polysaccharides including sulfated polysaccharides and non-sulfated neutral polysaccharides.

As shown in Fig. 3-11, a saturated δ value of imidazole H4,5 (7.485 ppm) in the presence of reduced polysaccharide derived from *M. nitidum* was observed up to 0.75 mmol-imidazole/g-reduced crude polysaccharide, whereas at > 0.75 mmol-imidazole/g-reduced crude polysaccharide a dose-dependent up-field shift of imidazole H4,5 was observed. Notably, as shown in Fig. 3-12, the observed δ value of imidazole showed a good linearity (R^2=0.985) against the concentration of imidazole in the range of 0.88–3.25 mmol-imidazole/g-reduced crude polysaccharide. The sulfate content in Aichi *M. nitidum* crude polysaccharide was estimated to be 0.79 mmol-imidazole/g-reduced crude polysaccharide (i.e., 7.61 wt%) from the molar concentration of imidazole at the predicted inflection point of the plot by the regression equation (Fig. 3-12). The estimated sulfate content by the proposed ^{1}H NMR assay was in agreement with that by the conventional barium-rhodizonate assay (7.94 ± 0.64 wt%) (Table 3-2). Besides, irrespective of geographic locations and species, for all seaweed samples, the estimated sulfate contents by the imidazole-assisted ^{1}H NMR assay were in the range of those predicted by the triplicate barium-rhodizonate assay (Fig. 3-12).

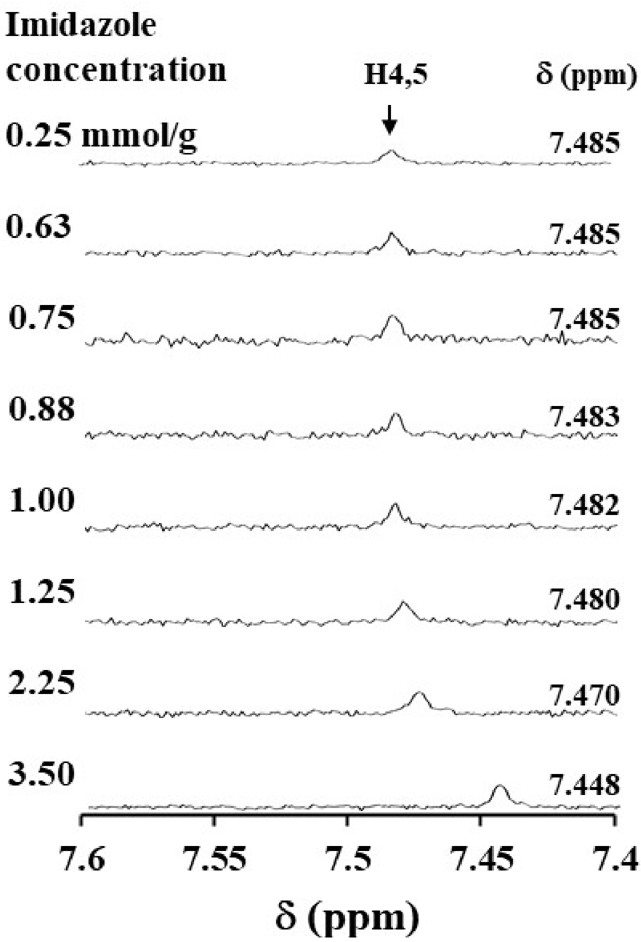

Fig. 3-11. Change in chemical shift (Δδ) of imidazole target protons (H4,5) at the different concentrations of imidazole in the chemical reduced polysaccharide extract from Aichi *Monostroma nitidum*.

A chemical reduction was performed according to the section of Materials and Methods. The concentration of reduced crude polysaccharide was fixed at 0.08 mg/mL. Different concentrations of imidazole were added at 0.25–3.5 mmol-imidazole/g-reduced crude polysaccharide.

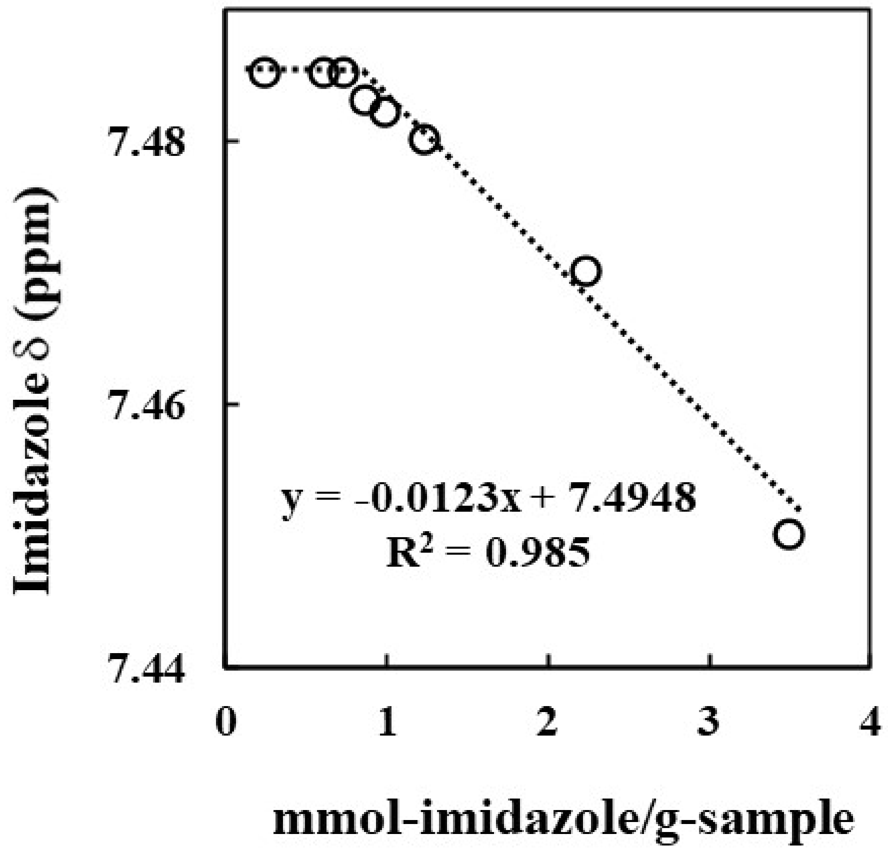

Fig. 3-12. A plot of chemical shift (δ) of imidazole target proton (H4,5) *vs.* concentrations of imidazole in the chemical reduced polysaccharide extract from Aichi *Monostroma nitidum*.

δ values of imidazole were obtained from the result of Fig. 3-11. The concentration of reduced crude polysaccharide was fixed at 0.08 mg/mL. Different concentrations of imidazole were added at 0.25–3.5 mmol-imidazole/g-reduced crude polysaccharide.

Table 3-2. Sulfate content in various seaweed polysaccharides obtained by imidazole-assisted ^{1}H NMR and barium-rhodizonate assays.

Seaweed		Harvest region	Sulfate content (wt%)	
Common name	Scientific name		^{1}H NMR assay	Barium-rhodizonate assay*
Aosa-Nori	*Monostroma nitidum*	Aichi	7.61	7.94 ± 0.64 (7.33–8.59)
Nori	*Porphyra yezoensis*	Shizuoka	7.41	7.50 ± 0.66 (7.09–8.26)
Akamoku	*Sargassum horneri*	Aichi	7.17	7.37 ± 0.75 (6.79–8.21)
		Miyagi	7.31	6.82 ± 0.77 (6.21–7.67)
		Mie	3.77	4.37 ± 0.59 (3.73–4.86)
		Nagasaki	4.61	5.01 ± 0.40 (4.57–5.36)
Gagome-Kombu	*Kjellmaniella crassifolia*	Sapporo	10.4	11.1 ± 1.18 (10.1–12.4)
Ishi-Mozuku	*Sphaerotrichia firma*	Aomori	9.68	9.67 ± 0.30 (9.49–10.0)
		Niigata	16.3	16.0 ± 1.80 (14.7–18.1)
Kombu	*Saccharina japonica*	Iwate	4.35	4.43 ± 0.78 (3.71–5.24)
Mekabu	Sporophyll of *Undaria pinnatifida*	Miyagi	3.73	4.23 ± 0.90 (3.36–5.15)
		Shimane	7.56	7.35 ± 0.87 (6.42–8.15)
Okinawa-Mozuku	*Cladosiphon okamuranus*	Ishigaki Island	4.81	5.35 ± 0.58 (4.68–5.68)
		Kume Island	4.04	4.32 ± 0.40 (3.94–4.72)
		Miyako Island	4.65	4.05 ± 0.71 (3.28–4.68)
		Tsuken Island	4.97	4.51 ± 0.82 (3.86–5.42)
Wakame	*Undaria pinnatifida*	Iwate	2.45	3.10 ± 0.83 (2.29–3.93)
		Miyagi	2.79	3.36 ± 0.95 (2.38–4.26)
		Nagasaki	5.53	5.77 ± 0.69 (5.02–6.35)
		Tokushima	3.85	3.70 ± 0.85 (2.74–4.33)

* Values indicate the mean ± SD (*n*=3); total value range from triplicated measurements is provided in parentheses.

4. Summary

Chapter III demonstrates for the first time that ^{1}H NMR can be used for the assay of sulfate content in saccharides by monitoring the $\Delta\delta$ of appropriate ligand. All the present findings strongly evidence that imidazole is the most applicable ligand to selectively form a stoichiometric complex with sulfate group in sulfated saccharides, irrespective to the presence of interfering non-sulfated saccharides. Because carboxy group in saccharides ionically interacted with imidazole, carboxy group in polysaccharides was eliminated by the chemical reduction prior to ^{1}H NMR measurement. The sulfate content of sulfated saccharides including natural polysaccharides is estimated by the molar concentration of imidazole at the predicted inflection point from the plot based on the observed δ values against the molar concentrations of imidazole. Therefore, the proposed ^{1}H NMR assay can be extensively utilized for estimating sulfate content in natural polysaccharides without destructive pretreatments, such as acid hydrolysis and intensive extraction.

Chapter IV

Conclusion

Sulfate groups in sulfated polysaccharides, particularly fucoidan, are considered as a key structural factor in exhibiting physiological activities, such as anti-tumor and immune-stimulation effects.[49-51] Previous studies have revealed that immune activation induced by fucoidan is triggered with the action of macrophage.[32,33] Agonistic binding of fucoidan to PRRs, expressed on cell membrane, stimulated macrophage to produce proinflammatory molecules such as TNF-α and NO.[35] In addition, fucoidan expected to cooperate with other ligands such as β-glucan to activate multiple cell surface receptors expressed on macrophage, and enhance their immune-stimulation activity.[14,48,94] However, due to an absence of clear information about fucoidan receptors and assay for sulfate content in natural sulfated polysaccharides without tedious extraction and pretreatment procedures, the involvement of sulfate group in physiological functions of fucoidan is still uncertain. Therefore, the goals of this study were to explore the synergistic immune response between fucoidan and β-

glucan via any receptor interaction (in **Chapter II**), and to establish a new assay for sulfate content estimation in seaweed polysaccharides (in **Chapter III)**.

Chapter II Synergistic immune-stimulation on macrophage activation by Okinawa-Mozuku (*Cladosiphon okamuranus*) fucoidan and β-glucan derived from *Saccharomyces cerevisiae* in RAW264 cells

In order to investigate the immune-stimulation effect of fucoidan, *C. okamuranus* fucoidan was used. RAW264 cells were used to assess macrophage function. In addition, zymosan (a well-known β-glucan-rich cell wall prepared from *S. cerevisiae*) was used for evaluating the synergistic effect between fucoidan and β-glucan.

As a result, fucoidan was visualized on the cell surface of RAW264 cells by CLSM, and was found to stimulate the production of NO and TNF-α without cellular internalization. The production of NO and TNF-α was enhanced by co-operative action of fucoidan and zymosan. Lipid rafts, which scaffold for rearrangement of PRRs, such as dectin-1 and TLRs during the activation of macrophage, were revealed to be involved in the synergistic immune-stimulation activity. Notably, dectin-1, one sort of β-glucan receptor, was essential for the synergistic effect between fucoidan and zymosan. Therefore, all findings indicate that fucoidan interacted with some receptors expressed on RAW264 cell membranes, and the fucoidan-activated receptors reinforced immune function by the cooperation with dectin-1 activated by zymosan.

Chapter III Ligand-assisted nuclear magnetic resonance (NMR) spectrometry assay for sulfate content in sulfated polysaccharides

In this chapter, an establishment of new assay for sulfate content in sulfated polysaccharides was performed applying ^{1}H NMR titration method.

First of all, among five candidates, imidazole, showing a well-resolved ^{1}H NMR signal largely shifted toward down-field in the presence of sulfated disaccharide (NB-*s*), was selected to explore a stoichiometric complex formation between ligand molecule and sulfate group in saccharides. The δ value of imidazole in the presence of NB-*s* was constant until molar ratios of imidazole to sulfate group were 1:1, whereas at > 1:1, a dose-dependent up-field shift of imidazole H4,5 signal was observed, indicating that imidazole formed the 1:1 stoichiometric complex with sulfate group in saccharides. In addition, a plot based on the observed δ values of imidazole against the molar ratios of imidazole to sulfate group in saccharides can allow to estimate sulfate content in sulfated saccharides. Namely, when observed δ values of imidazole in the presence of sulfated saccharides were schematized against molar concentrations of imidazole, molar concentration of imidazole at the inflection point of the plot may correspond to sulfate content in saccharides.

Next, the application of an imidazole-assisted ^{1}H NMR assay to estimate sulfate content in seaweed polysaccharides was performed. The interference of non-sulfated saccharides composing seaweed polysaccharides was investigated on a 1:1 binding stoichiometry between imidazole and sulfate group in saccharides. For that purpose, non-sulfated neutral saccharides (mono- to tetra-saccharides) and carboxylated saccharide (galacturonic acid) were used. As a result, the presence of non-sulfated neutral saccharides did not affect the stoichiometric complex formation. Galacturonic acid ionically interacted with imidazole, whereas the interaction was abolished by removing carboxyl group in saccharide. Therefore, to apply a ligand-assisted ^{1}H NMR assay for the estimation of sulfate content in seaweed polysaccharides, carboxy group in crude polysaccharides was eliminated prior to ^{1}H NMR measurement by removal of alginate (highly carboxylated seaweed polysaccharide) and subsequent chemical reduction to form hydroxymethyl group. The chemically reduced polysaccharides extracted from twenty seaweeds spanning nine species and various geographic locations were used as analytes for the proposed ^{1}H NMR assay to estimate sulfate contents in natural crude polysaccharides. Exceptionally, the estimation of sulfate content in commercially available fucoidan derived from *F. vesiculosus* was achieved without the chemical reduction procedure due to no carboxy groups. The estimated sulfate contents of all tested samples by the proposed imidazole-assisted ^{1}H NMR assay were matched with those by a conventional barium-rhodizonate assay. These results indicated that imidazole was an appropriate ligand to form 1:1 stoichiometric complex with sulfate group in sulfated polysaccharides, and the proposed imidazole-assisted ^{1}H NMR assay can be extensively applied to estimate sulfate content in various natural polysaccharides with appropriate pretreatment to eliminate carboxy groups.

In conclusion, the present study demonstrates for the first time that fucoidan cooperates with β-glucan to activate multiple receptors on lipid rafts and enhances immune activity of macrophage. In addition, the findings prove that the ligand-assisted ^{1}H NMR method using imidazole as a ligand can be extensively applied for estimating sulfate content in various sulfated saccharides including natural polysaccharides prepared without destructive preparation steps.

References

[1] Penesyan, A.; Kjelleberg, S.; Egan, S. Development of novel drugs from marine surface associated microorganisms. *Mar. Drugs* **2010**, *8*, 438–459.

[2] Silva, T. H.; Alves, A.; Popa, E. G.; Reys, L. L.; Gomes, M. E.; Sousa, R. A.; Silva, S. S.; Mano, J. F.; Reis, R. L. Marine algae sulfated polysaccharides for tissue engineering and drug delivery approaches. *Biomatter* **2012**, *2*, 278–289.

[3] Gómez-Guzmán, M.; Rodríguez-Nogales, A.; Algieri, F.; Gálvez, J. Potential role of seaweed polyphenols in cardiovascular-associated disorders. *Mar. Drugs* **2018**, *16*, 250.

[4] Patel, S. Therapeutic importance of sulfated polysaccharides from seaweeds: updating the recent findings. *3 Biotech* **2012**, *2*, 171–185.

[5] Ale, M. T.; Mikkelsen, J. D.; Meyer, A. S. Important determinants for fucoidan bioactivity: a critical review of structure-function relations and extraction methods for fucose-containing sulfated polysaccharides from brown seaweeds. *Mar. Drugs* **2011**, *9*, 2106–2130.

[6] Mohamed, S.; Hashim, S. N.; Rahman, H. A. Seaweeds: a sustainable functional food for complementary and alternative therapy. *Trends Food Sci. Technol.* **2012**,

23, 83–96.

[7] Jin, J. O.; Zhang, W.; Du, J. Y.; Wong, K. W.; Oda, T.; Yu, Q. Fucoidan can function as an adjuvant in vivo to enhance dendritic cell maturation and function and promote antigen-specific T cell immune responses. *PLoS One* **2014**, *9*, e99396.

[8] Kawashima, T.; Murakami, K.; Nishimura, I.; Nakano, T.; Obata, A. A sulfated polysaccharide, fucoidan, enhances the immunomodulatory effects of lactic acid bacteria. *Int. J. Mol. Med.* **2012**, *29*, 447–453.

[9] Maruyama, H.; Tamauchi, H.; Hashimoto, M.; Nakano, T. Antitumor activity and immune response of Mekabu fucoidan extracted from Sporophyll of *Undaria pinnatifida*. *In Vivo* **2003**, *17*, 245–249.

[10] Xue, M.; Ge, Y.; Zhang, J.; Wang, Q.; Hou, L.; Liu, Y.; Sun, L.; Li, Q. Anticancer properties and mechanisms of fucoidan on mouse breast cancer in vitro and in vivo. *PLoS One* **2012**, *7*, e43483.

[11] Usoltseva, R. V.; Anastyuk, S. D.; Surits, V. V.; Shevchenko, N. M.; Thinh, P. D.; Zadorozhny, P. A.; Ermakova, S. P. Comparison of structure and in vitro anticancer activity of native and modified fucoidans from *Sargassum feldmannii* and *S. duplicatum*. *Int. J. Biol. Macromol.* **2019**, *124*, 220–228.

[12] Aisa, Y.; Miyakawa, Y.; Nakazato, T.; Shibata, H.; Saito, K.; Ikeda, Y.; Kizaki, M. Fucoidan induces apoptosis of human HS-sultan cells accompanied by activation of caspase-3 and down-regulation of ERK pathways. *Am. J. Hematol.*

2005, *78*, 7–14.

[13] Cho, M. L.; Lee, B. Y.; You, S. G. Relationship between oversulfation and conformation of low and high molecular weight fucoidans and evaluation of their in vitro anticancer activity. *Molecules* **2011**, *16*, 291–297.

[14] Ferwerda, G.; Meyer-Wentrup, F.; Kullberg, B. J.; Netea, M. G.; Adema, G. J. Dectin-1 synergizes with TLR2 and TLR4 for cytokine production in human primary monocytes and macrophages. *Cell. Microbiol.* **2008**, *10*, 2058–2066.

[15] Kasai, A.; Arafuka, S.; Koshiba, N.; Takahashi, D.; Toshima, K. Systematic synthesis of low-molecular weight fucoidan derivatives and their effect on cancer cells. *Org. Biomol. Chem.* **2015**, *13*, 10556-10568.

[16] Yang, L.; Wang, P.; Wang, H.; Li, Q.; Teng, H.; Liu, Z.; Yang, W.; Hou, L.; Zou, X. Fucoidan derived from Undaria pinnatifida induces apoptosis in human hepatocellular carcinoma SMMC-7721 cells via the ROS-mediated mitochondrial pathway. *Mar. Drugs* **2013**, *11*, 1961–1976.

[17] Melo, M. R. S.; Feitosa, J. P. A.; Freitas, A. L. P.; De Paula, R. C. M. Isolation and characterization of soluble sulfated polysaccharide from the red seaweed *Gracilaria cornea*. *Carbohydr. Polym.* **2002**, *49*, 491–498.

[18] Li, B.; Lu, F.; Wei, X.; Zhao, R. Fucoidan: structure and bioactivity. *Molecules* **2008**, *13*, 1671–1695.

[19] Oliveira, C.; Neves, N. M.; Reis, R. L.; Martins, A.; Silva, T. H. A review on fucoidan antitumor strategies: from a biological active agent to a structural component of fucoidan-based systems. *Carbohydr. Polym.* **2020**, *239*, 116131.

[20] Zhao, Y.; Zheng, Y.; Wang, J.; Ma, S.; Yu, Y.; White, W. L.; Yang, S.; Yang, F.; Lu, J. Fucoidan extracted from *Undaria pinnatifida*: Source for nutraceuticals/functional foods. *Mar. Drugs* **2018**, *16*, 321.

[21] Lin, Y.; Zhang, L.; Chen, L.; Jin, Y.; Zeng, F.; Jin, J.; Wan, B.; Cheung, P. C. K. Molecular mass and antitumor activities of sulfated derivatives of α-glucan from *Poria cocos* mycelia *Int. J. Biol. Macromol.* **2004**, *34*, 231–236.

[22] Oka, S.; Okabe, M.; Tsubura, S.; Mikami, M.; Imai, A. Properties of fucoidans beneficial to oral healthcare. *Odontology* **2020**, *108*, 34–42.

[23] Cunha, L.; Grenha, A. Sulfated seaweed polysaccharides as multifunctional materials in drug delivery applications. *Mar. Drugs* **2016**, *14*, 42.

[24] Koyanagi, S.; Tanigawa, N.; Nakagawa, H.; Soeda, S.; Shimeno, H. Oversulfation of fucoidan enhances its anti-angiogenic and antitumor activities. *Biochem. Pharmacol.* **2003**, *65*, 173–179.

[25] Haroun-Bouhedja, F.; Ellouali, M.; Sinquin, C.; Boisson-Vidal, C. Relationship between sulfate groups and biological activities of fucans. *Thromb. Res.* **2000**, *100*, 453–459.

[26] Koh, H. S. A.; Lu, J.; Zhou, W. Structure characterization and antioxidant activity of fucoidan isolated from *Undaria pinnatifida* grown in New Zealand. *Carbohydr. Polym.* **2019**, *212*, 178–185.

[27] Ale, M. T.; Meyer, A. S. Fucoidans from brown seaweeds: An update on structures, extraction techniques and use of enzymes as tools for structural elucidation. *RSC Adv.* **2013**, *3*, 8131–8141.

[28] Oliveira, C.; Ferreira, A. S.; Novoa-Carballal, R.; Nunes, C.; Pashkuleva, I.; Neves, N. M.; Coimbra, M. A.; Reis, R. L.; Martins, A.; Silva, T. H. The key role of sulfation and branching on fucoidan antitumor activity. *Macromol. Biosci.* **2017**, *17*, 1600340.

[29] You, S.; Yang, C.; Lee, H.; Lee, B. Molecular characteristics of partially hydrolyzed fucoidans from sporophyll of *Undaria pinnatifida* and their in vitro anticancer activity. *Food Chem.* **2010**, *119*, 554–559.

[30] Nagaoka, M.; Shibata, H.; Kimura-Takagi, I.; Hashimoto, S.; Kimura, K.; Makino, T.; Aiyama, R.; Ueyama, S.; Yokokura, T. Structural study of fucoidan from *Cladosiphon okamuranus* Tokida. *Glycoconj. J.* **1999**, *16*, 19–26.

[31] Nishino, T.; Aizu, Y.; Nagumo, T. The influence of sulfate content and molecular weight of a fucan sulfate from the brown seaweed *Ecklonia kurome* on its antithrombin activity. *Thromb. Res.* **1991**, *64*, 723–731.

[32] Park, S. Y.; Hwang, E.; Shin, Y. K.; Lee, D. G.; Yang, J. E.; Park, J. H.; Yi, T. H.

Immunostimulatory effect of enzyme-modified *Hizikia fusiforme* in a mouse model in vitro and ex vivo. *Mar. Biotechnol.* **2017**, *19*, 65–75.

[33] Takeda, K.; Tomimori, K.; Kimura, R.; Ishikawa, C.; Nowling, T. K.; Mori, N. Anti-tumor activity of fucoidan is mediated by nitric oxide released from macrophages. *Int. J. Oncol.* **2012**, *40*, 251–260.

[34] Gordon, S. Alternative activation of macrophages. *Nat. Rev. Immunol.* **2003**, *3*, 23–35.

[35] Lin, Z.; Tan, X.; Li, F.; Luo, P.; Liu, H. Molecular targets and related biologic activities of fucoidan: A review *Mar. Drugs* **2020**, *18*, 376.

[36] Kim, Y. S.; Ryu, J. H.; Han, S. J.; Choi, K. H.; Nam, K. B.; Jang, I. H.; Lemaitre, B.; Brey, P. T.; Lee, W. J. Gram-negative bacteria-binding protein, a pattern recognition receptor for lipopolysaccharide and β-1, 3-glucan that mediates the signaling for the induction of innate immune genes in *Drosophila melanogaster* cells. *J. Biol. Chem.* **2000**, *275*, 32721–32727.

[37] Akira, S.; Takeda, K. Toll-like receptor signalling. *Nat. Rev. Immunol.* **2004**, *4*, 499–511.

[38] Akira, S.; Uematsu, S.; Takeuchi, O. Pathogen recognition and innate immunity. *Cell* **2006**, *124*, 783–801.

[39] Manne, B. K.; Getz, T. M.; Hughes, C. E.; Alshehri, O.; Dangelmaier, C.; Naik,

U. P.; Watson, S. P.; Kunapuli, S. P. Fucoidan is a novel platelet agonist for the C-type lectin-like receptor 2 (CLEC-2). *J. Biol. Chem.* **2013**, *288*, 7717–7726.

[40] Hsu, H. Y.; Lin, T. Y.; Lu, M. K.; Leng, P. J.; Tsao, S. M.; Wu, Y. C. Fucoidan induces Toll-like receptor 4-regulated reactive oxygen species and promotes endoplasmic reticulum stress-mediated apoptosis in lung cancer. *Sci. Rep.* **2017**, *7*, 44990.

[41] Nakamura, T.; Suzuki, H.; Wada, Y.; Kodama, T.; Doi, T. Fucoidan induces nitric oxide production via p38 mitogen-activated protein kinase and NF-κB-dependent signaling pathways through macrophage scavenger receptors. *Biochem. Biophys. Res. Commun.* **2006**, *343*, 286–294.

[42] Yu, H.; Ha, T.; Liu, L.; Wang, X.; Gao, M.; Kelley, J.; Kao, R.; Williams, D.; Li, C. Scavenger receptor A (SR-A) is required for LPS-induced TLR4 mediated NF-κB activation in macrophages. *Biochim. Biophys. Acta* **2012**, *1823*, 1192–1198.

[43] Teruya, T.; Tatemoto, H.; Konishi, T.; Tako, M. Structural characteristics and in vitro macrophage activation of acetyl fucoidan from *Cladosiphon okamuranus*. *Glycoconj. J.* **2009**, *26*, 1019–1028.

[44] Wenner, C. A.; Güler, M. L.; Macatonia, S. E.; O'Garra, A.; Murphy, K. M. Roles of IFN-gamma and IFN-alpha in IL-12-induced T helper cell-1 development. *J. Immunol.* **1996**, *156*, 1442–1447.

[45] Wang, R.; Jaw, J. J.; Stutzman, N. C.; Zou, Z.; Sun, P. D. Natural killer cell-

produced IFN-γ and TNF-α induce target cell cytolysis through up-regulation of ICAM-1. *J. Leukoc. Biol.* **2012**, *91*, 299–309.

[46] Sato, S.; Nomura, F.; Kawai, T.; Takeuchi, O.; Mühlradt, P. F.; Takeda, K.; Akira, S. Synergy and cross-tolerance between toll-like receptor (TLR) 2-and TLR4-mediated signaling pathways. *J. Immunol.* **2000**, *165*, 7096–7101.

[47] Underhill, D. M. Collaboration between the innate immune receptors dectin-1, TLRs, and Nods. *Immunol. Rev.* **2007**, *219*, 75-87.

[48] Dennehy, K. M.; Ferwerda, G.; Faro-Trindade, I.; Pyż, E.; Willment, J. A.; Taylor, P. R.; Kerrigna, A.; Vicky Tsoni, S.; Gordon, S.; Meyer-Wentrup, F.; Adema, G. J.; Kullberg, B. J.; Schweighoffer, E.; Tybulewicz , V.; Mora-Montes, H. M.; Gow, N. A. R.; Williams, D. L.; Netea, M. G.; Brown, G. D. Syk kinase is required for collaborative cytokine production induced through Dectin-1 and Toll-like receptors. *Eur. J. Immunol.* **2008**, *38*, 500–506.

[49] Wang, X.; Zhang, L. Physicochemical properties and antitumor activities for sulfated derivatives of lentinan. *Carbohydr. Res.* **2009**, *344*, 2209–2216.

[50] Patankar, M. S.; Oehninger, S.; Barnett, T.; Williams, R. L.; Clark, G. F. A revised structure for fucoidan may explain some of its biological activities. *J. Biol. Chem.* **1993**, *268*, 21770–21776.

[51] Sun, Y.; Gong, G.; Guo, Y.; Wang, Z.; Song, S.; Zhu, B.; Zhao, L.; Jiang, J. Purification, structural features and immunostimulatory activity of novel

polysaccharides from *Caulerpa lentillifera*. *Int. J. Biol. Macromol.* **2018**, *108*, 314–323.

[52] Jun, J. Y.; Jung, M. J.; Jeong, I. H.; Yamazaki, K.; Kawai, Y.; Kim, B. M. Antimicrobial and antibiofilm activities of sulfated polysaccharides from marine algae against dental plaque bacteria. *Mar. Drugs* **2018**, *16*, 301.

[53] Qiao, D.; Luo, J.; Ke, C.; Sun, Y.; Ye, H.; Zeng, X. Immunotimulatory activity of the polysaccharides from *Hyriopsis cumingii*. *Int. J. Biol. Macromol.* **2010**, *47*, 676–680.

[54] Ale, M. T.; Mikkelsen, J. D.; Meyer, A. S. Designed optimization of a single-step extraction of fucose-containing sulfated polysaccharides from *Sargassum* sp. *J. Appl. Phycol.* **2011**, *24*, 715–723.

[55] Wang, C. Y.; Chen, Y. C. Extraction and characterization of fucoidan from six brown macroalgae. *J. Mar. Sci. Technol.* **2016**, *24*, 319–328.

[56] Hahn, T.; Lang, S.; Ulber, R.; Muffler, K. Novel procedures for the extraction of fucoidan from brown algae. *Process Biochem.* **2012**, *47*, 1691–1698.

[57] Wang, H.; Liu, X.; Nan, K.; Chen, B.; He, M.; Hu, B. Sample pre-treatment techniques for use with ICP-MS hyphenated techniques for elemental speciation in biological samples. *J. Anal. Atomic Spectrom.* **2017**, *32*, 58–77.

[58] Rioux, L. E.; Turgeon, S. L.; Beaulieu, M. Rheological characterisation of

polysaccharides extracted from brown seaweeds. *J. Sci. Food Agric.* **2007**, *87*, 1630–1638.

[59] de la Rocha, S. R.; Sánchez-Muniz, F. J.; Gómez-Juaristi, M.; Marín, M. L. Trace elements determination in edible seaweeds by an optimized and validated ICP-MS method. *J. Food Compost. Anal.* **2009**, *22*, 330–336.

[60] Karlsson, A.; Singh, S. K. Acid hydrolysis of sulphated polysaccharides. Desulphation and the effect on molecular mass. *Carbohydr. Polym.* **1999**, *38*, 7-15.

[61] Rochas, C.; Lahaye, M.; Yaphe, W. Sulfate content of carrageenan and agar determined by infrared spectroscopy. *Bot. Mar.* **1986**, *29*, 335–340.

[62] De Gussem, K.; Vandenabeele, P.; Verbeken, A.; Moens, L. Raman spectroscopic study of *Lactarius spores* (Russulales, Fungi). *Spectrochim. Acta, Pt. A: Mol. Biomol. Spectrosc.* **2005**, *61*, 2896–2908.

[63] Sharma, R.; Gupta, P. K.; Mazumder, A.; Dubey, D. K.; Ganesan, K.; Vijayaraghavan, R. A quantitative NMR protocol for the simultaneous analysis of atropine and obidoxime in parenteral injection devices. *J. Pharm. Biomed. Anal.* **2009**, *49*, 1092–1096.

[64] Forshed, J.; Erlandsson, B.; Jacobsson, S. P. Quantification of aldehyde impurities in poloxamer by ^{1}H NMR spectrometry. *Anal. Chim. Acta* **2005**, *552*, 160–165.

[65] Marcone, M. F.; Wang, S.; Albabish, W.; Nie, S.; Somnarain, D.; Hill, A. Diverse food-based applications of nuclear magnetic resonance (NMR) technology. *Food Res. Int.* **2013**, *51*, 729–747.

[66] Wu, Z.; Ming, J.; Gao, R.; Wang, Y.; Liang, Q.; Yu, H.; Zhao, G. Characterization and antioxidant activity of the complex of tea polyphenols and oat β-glucan. *J. Agric. Food Chem.* **2011**, *59*, 10737–10746.

[67] Cao, R.; Komura, F.; Nonaka, A.; Kato, T.; Fukumashi, J.; Matsui, T. Quantitative analysis of D-(+)-glucose in fruit juices using diffusion ordered-^{1}H nuclear magnetic resonance spectroscopy. *Anal. Sci.* **2014**, *30*, 383–388.

[68] Cao, R.; Nonaka, A.; Komura, F.; Matsui, T. Application of diffusion ordered-^{1}H-nuclear magnetic resonance spectroscopy to quantify sucrose in beverages. *Food Chem.* **2015**, *171*, 8–12.

[69] Schievano, E.; Tonoli, M.; Rastrelli, F. NMR quantification of carbohydrates in complex mixtures. A challenge on honey. *Anal. Chem.* **2017**, *89*, 13405–13414.

[70] Kato, T.; Abe, A.; Miyadera, A.; Yamamoto, K.; Harada, T.; Ito, H.; Miizukoshi, K.; Igarashi, T. Non-destructive quantification method for glucans using proton qunatitative nuclear magnetic resonance spectroscopy. *J. Jpn. Soc. Food Sci. Technol.* **2020**, *67*, 430–441 (in Japanese).

[71] Berregi, I.; del Campo, G.; Caracena, R.; Miranda, J. I. Quantitative determination of formic acid in apple juices by ^{1}H NMR spectrometry. *Talanta*

2007, *72*, 1049–1053.

[72] Colnago, L. A.; Azeredo, R. B. V.; Marchi Netto, A.; Andrade, F. D.; Venâncio, T. Rapid analyses of oil and fat content in agri-food products using continuous wave free precession time domain NMR. *Magn. Reson. Chem.* **2011**, *49*, S113–S120.

[73] Jame, T. L. Fundamentals of NMR. Chapter 1 Biophysics Textbook Online. Biophysical Society. Maryland, 1998, 1–31.

[74] Hanson, L. G. Is quantum mechanics necessary for understanding magnetic resonance? *Concepts Magn. Reson. A: Bridg. Educ. Res.* **2008**, *32*, 329–340.

[75] Ernst, R. R.; Anderson, W. A. Application of Fourier transform spectroscopy to magnetic resonance. *Rev. Sci. Instrum.* **1966**, *37*, 93–102.

[76] Abragam, A. Principles of nuclear magnetism. Oxford University Press. Oxford, 1961.

[77] Saito, T.; Ihara, T.; Koike, M.; Kinugasa, S.; Fujimine, Y.; Nose, K.; Hirai, T. A new traceability scheme for the development of international system-traceable persistent organic pollutant reference materials by quantitative nuclear magnetic resonance. *Accredit. Qual. Assur.* **2009**, *14*, 79–86.

[78] Cheng, H. N.; Neiss, T. G. Solution NMR spectroscopy of food polysaccharides. *Polym. Rev.* **2012**, *52*, 81–114.

[79] Sprangers, R.; Groves, M. R.; Sinning, I.; Sattler, M. High-resolution X-ray and NMR structures of the SMN Tudor domain: conformational variation in the binding site for symmetrically dimethylated arginine residues. *J. Mol. Biol.* **2003**, *327*, 507–520.

[80] Fielding, L.; Rutherford, S.; Fletcher, D. Determination of protein–ligand binding affinity by NMR: observations from serum albumin model systems. *Magn. Reson. Chem.* **2005**, *43*, 463–470.

[81] Jia, C.; Wu, B.; Li, S.; Huang, X.; Zhao, Q.; Li, Q. S.; Yang, X. J. Highly efficient extraction of sulfate ions with a tripodal hexaurea receptor. *Angew. Chem.* **2011**, *123*, 506–510.

[82] Khansari, M. E.; Hasan, M. H.; Johnson, C. R.; Williams, N. A.; Wong, B. M.; Powell, D. R.; Tandon, R.; Hossain, M. A. Anion complexation studies of 3-nitrophenyl-substituted tripodal thiourea receptor: A naked-eye detection of sulfate via fluoride displacement assay. *ACS Omega* **2017**, *2*, 9057–9066.

[83] Berger, M.; Schmidtchen, F. P. The binding of sulfate anions by guanidinium receptors is entropy-driven. *Angew. Chem. Int. Ed.* **1998**, *37*, 2694–2696.

[84] Jin, C.; Zhang, M.; Wu, L.; Guan, Y.; Pan, Y.; Jiang, J.; Lin, C.; Wang, L. Squaramide-based tripodal receptors for selective recognition of sulfate anion. *Chem. Commun.* **2013**, *49*, 2025–2027.

[85] Sato, K.; Onitake, T.; Arai, S. Size selective recognition of anions by a tetracationic imidazoliophane. *Heterocylces* **2003**, *60*, 779–784.

[86] Ihm, H.; Yun, S.; Kim, H. G.; Kim, J. K.; Kim, K. S. Tripodal nitro-imidazolium receptor for anion binding driven by $(C-H)^{+}$---X^{-}hydrogen bonds. *Org. Lett.* **2002**, *4*, 2897–2900.

[87] Yoon, J.; Kim, S. K.; Singh, N. J.; Kim, K. S. Imidazolium receptors for the recognition of anions. *Chem. Soc. Rev.* **2006**, *35*, 355–360.

[88] In, S.; Cho, S. J.; Kang, J. Anion receptor with xylene bridged two imidazolium rings. *Supramol. Chem.* **2005**, *17*, 443–446.

[89] Wu, L.; Sun, J.; Su, X.; Yu, Q.; Yu, Q.; Zhang, P. A review about the development of fucoidan in antitumor activity: Progress and challenges. *Carbohydr. Polym.* **2016**, *154*, 96–111.

[90] Song, Y.; Wang, Q.; Wang, Q.; He, Y.; Ren, D.; Liu, S.; Wu, L. Structural characterization and antitumor effects of fucoidans from brown algae *Kjellmaniella crassifolia* farmed in northern China. *Int. J. Biol. Macromol.* **2018**, *119*, 125–133.

[91] Karnjanapratum, S.; You, S. Molecular characteristics of sulfated polysaccharides from *Monostroma nitidum* and their in vitro anticancer and immunomodulatory activities. *Int. J. Biol. Macromol.* **2011**, *48*, 311–318.

[92] Kar, S.; Sharma, G.; Das, P. K. Fucoidan cures infection with both antimony-susceptible and-resistant strains of *Leishmania donovani* through Th1 response and macrophage-derived oxidants. *J. Antimicrob. Chemother.* **2011**, *66*, 618–625.

[93] Maruyama, H.; Tamauchi, H.; Iizuka, M.; Nakano, T., 1415-7. The role of NK cells in antitumor activity of dietary fucoidan from *Undaria pinnatifida*. *Planta Med.* **2006**, *7*, 1415–1417.

[94] Gantner, B. N.; Simmons, R. M.; Canavera, S. J.; Akira, S.; Underhill, D. M. Collaborative induction of inflammatory responses by dectin-1 and Toll-like receptor 2. *J. Exp. Med.* **2003**, *197*, 1107–1117.

[95] Shamsul, H. M.; Hasebe, A.; Lyori, M.; Ohtani, M.; Kiura, K.; Zhang, D.; Totsuka, Y.; Shibata, K. I. T. The Toll-like receptor 2 (TLR2) ligand FSL-1 is internalized via the clathrin-dependent endocytic pathway triggered by CD14 and CD36 but not by TLR2. *Immunology* **2010**, *130*, 262–272.

[96] Herre, J.; Marshall, A. S.; Caron, E.; Edwards, A. D.; Williams, D. L.; Schweighoffer, E.; Tybulewicz , V.; Reis e Sousa, C.; Gordon, S.; Brown, G. D. Dectin-1 uses novel mechanisms for yeast phagocytosis in macrophages. *Blood* **2004**, *104*, 4038–4045.

[97] Yin, M.; Zhang, Y.; Li, H. Advances in research on immunoregulation of macrophages by plant polysaccharides. *Front. Immunol.* **2019**, *10*, 145.

[98] Qi, C.; Cai, Y.; Gunn, L.; Ding, C.; Li, B.; Kloecker, G.; Qian, K.; vasilakos, J.; Saijo, S.; Iwakura, Y.; Yannelli, J. R.; Yan, J. Differential pathways regulating innate and adaptive antitumor immune responses by particulate and soluble yeast-derived β-glucans. *Blood* **2011**, *117*, 6825–6836.

[99] Huang, J. H.; Lin, C. Y.; Wu, S. Y.; Chen, W. Y.; Chu, C. L.; Brown, G. D.; Chuu, C. P.; Wu-Hsieh, B. A. CR3 and Dectin-1 collaborate in macrophage cytokine response through association on lipid rafts and activation of Syk-JNK-AP-1 pathway. *PLoS Pathogens* **2015**, *11*, e1004985.

[100] Shin, D. M.; Yang, C. S.; Lee, J. Y.; Lee, S. J.; Choi, H. H.; Lee, H. M.; Yuk, J. M.; Harding, C. V.; Jo, E. K. Mycobacterium tuberculosis lipoprotein-induced association of TLR2 with protein kinase C zeta in lipid rafts contributes to reactive oxygen species-dependent inflammatory signalling in macrophages. *Cell. Microbiol.* **2008**, *10*, 1893–1905.

[101] Xu, S.; Huo, J.; Gunawan, M.; Su, I. H.; Lam, K. P. Activated dectin-1 localizes to lipid raft microdomains for signaling and activation of phagocytosis and cytokine production in dendritic cells. *J. Biol. Chem.* **2009**, *284*, 22005–22011.

[102] Sun, J.; Sun, J.; Song, B.; Zhang, L.; Shao, Q.; Liu, Y.; Yuan, D.; Zhang, Y.; Qu, X. Fucoidan inhibits CCL22 production through NF-κB pathway in M2 macrophages: a potential therapeutic strategy for cancer. *Sci. Rep.* **2016**, *6*, 35855.

[103] Mansour, M. B.; Balti, R.; Yacoubi, L.; Ollivier, V.; Chaubet, F.; Maaroufi, R.

M. Primary structure and anticoagulant activity of fucoidan from the sea cucumber *Holothuria polii*. *Int. J. Biol. Macromol.* **2019**, *121*, 1145–1153.

[104] Korva, H.; Kärkkäinen, J.; Lappalainen, K.; Lajunen, M. Spectroscopic study of natural and synthetic polysaccharide sulfate structures. *Starch-Stärke* **2016**, *68*, 854–863.

[105] Gale, P. A.; Hiscock, J. R.; Jie, C. Z.; Hursthouse, M. B.; Light, M. E. Acyclic indole and carbazole-based sulfate receptors. *Chem. Sci.* **2010**, *1*, 215–220.

[106] Lacey, M. E.; Subramanian, R.; Olson, D. L.; Webb, A. G.; Sweedler, J. V. High-resolution NMR spectroscopy of sample volumes from 1 nL to 10 μL. *Chem. Rev.* **1999**, *99*, 3133–3152.

[107] Jansen, E. F.; Jang, R. Esterification of galacturonic acid and polyuronides with methanol-hydrogen chloride. *J. Am. Chem. Soc.* **1946**, *68*, 1475–1477.

[108] Black, W. A. P.; Dewar, E. T.; Woodward, F. N. Manufacturing of algal chemicals 4: Laboratory scale isolation of fucoidan from brown marine algae. *J. Sci. Food Agric.* **1952**, *3*, 122–129.

[109] Silvestri, L. J.; Hurst, R. E.; Simpson, L.; Settine, J. M. Analysis of sulfate in complex carbohydrates. *Anal. Biochem.* **1982**, *123*, 303–309.

[110] Domenici, V. Dynamics in the isotropic and nematic phases of bent-core liquid crystals: NMR perspectives. *Soft Matter* **2011**, *7*, 1589–1598.

[111] Garna, H.; Emaga, T. H.; Robert, C.; Paquot, M. New method for the purification of electrically charged polysaccharides. *Food Hydrocoll.* **2011**, *25*, 1219–1226.

[112] Bittkau, K. S.; Neupane, S.; Alban, S. Initial evaluation of six different brown algae species as source for crude bioactive fucoidans. *Algal Res.* **2020**, *45*, 101759.

[113] Secouard, S.; Grisel, M.; Malhiac, C. Flavour release study as a way to explain xanthan–galactomannan interactions. *Food Hydrocoll.* **2007**, *21*, 1237–1244.

Acknowledgements

My doctoral dissertation was supported by many people, and it is not surprised that I would not finish my thesis without their supports. First of all, I would love to express my gratitude to Prof. Toshiro Matsui, who continuously supported me to do my own research during Ph.D. study. Thanks to his teachings and advice, I was able to reflect not only on what research is but also on how to live my life as a researcher. I am still lacking so much but, I would like to repay his teachings by trying hard to keep improving myself.

I am obliged to Assoc. Professor Yoshiyuki Miyazaki, who taught me various experimental techniques and knowledge while experimenting together and listened carefully to even the worst opinions, and I am very grateful for his scientific review for my doctoral thesis. In addition to him, I appreciate to Assoc. Professor Nozomu Okino for his professional review and good suggestions for my thesis too.

I would like to thank Assoc. Professor Mitsuru Tanaka and Ms. Kaori Miyazaki, who have been generous in helping me to live a stable life in Japan. I also would like to thank my colleagues in the lab who have been studying with me for the past three years and wish them good luck in the future.

I must thank the Japan Society for the Promotion of Science for its financial support for my research as well as daily life in Japan.

Besides those who are in Japan, I would like to take this opportunity to say thank you to my acquaintances in Korea. First and foremost, I want to say thank you and love you to my parents and older brother who always believed and supported my choice. Without their active supports, I would not have the courage to start my Ph.D. study in Japan.

Furthermore, I want to express my deep gratitude to Prof. Byoungseung Yoo of Dongguk University, who had supervised me from Undergraduate to Master study and still gives me a sincere advice for my future. Besides him, I'm grateful for alumni of Food Rheology and Processing lab in Dongguk University, who had studied together.

Lastly, I dedicate this thesis to my maternal grandfather, who passed away about two years ago and is now watching from heaven, with a word that I apology for not being able to stay his deathbed and attend his funeral.